

Ruderman-Kittel-Kasuya-Yosida (RKKY) interaction in Weyl semimetals with tilted energy dispersion

Anirban Kundu^{1,2} and M. B. A. Jalil¹

¹*Department of Electrical and Computer Engineering,
National University of Singapore, 4 Engineering Drive 3, Singapore 117576*

²*Physics Department, Ariel University, Ariel 40700, Israel*
(Dated: February 10, 2022)

Ruderman-Kittel-Kasuya-Yosida (RKKY) is an essential long range magnetic interaction between magnetic impurities or magnetic layered structures, the magnitude of which oscillates with the distance (R) between them. We have investigated the RKKY interaction between two magnetic impurities in both time-reversal and inversion symmetry broken Weyl semimetals (WSMs) where the energy dispersion is tilted in momentum space and the momentum of the conduction electron is locked with the pseudo-spin. Two important features are revealed, firstly, at the small tilt limit, we show that the RKKY coupling varies quadratically with the tilt parameter and strikingly, at large separation distance R , the coupling decays as $1/R$ compared to the conventional of $1/R^3$ dependence exhibited by WSMs with non-tilted dispersion. The slower decay by two orders i.e. ($1/R$ as opposed to $1/R^3$) of the RKKY coupling is significant for maintaining long range RKKY coupling. Secondly, the RKKY coupling exhibits an anisotropy with respect to the angle between the tilt direction (\mathbf{w}) and the separation direction \mathbf{R} unlike the case of non-tilted WSMs which exhibit isotropic RKKY coupling. Consequently, the RKKY coupling in tilted WSMs alternately favours ferromagnetic and anti-ferromagnetic orders and vice-versa with the change of the angle. Our results are derived analytically and verified by numerical calculations based on realistic parameter values.

I. INTRODUCTION

Recent progress on the study of various exotic topological materials and their transport properties has made Weyl semimetals a fascinating subject to study. A Weyl semimetal (WSM) can be produced from a four-fold degenerate Dirac semi-metal by breaking either or both of the time-reversal (TRS)/inversion-broken (IR) symmetry [1, 2]. In Dirac semi-metals, the band touching points known as nodes are four-fold degenerate and protected by TRS and IR symmetries. By breaking at least one of these symmetries, a pair of Weyl nodes is produced. The nodes harbor opposite topologically protected chiral charge η ($\eta = \pm 1, \pm 2, \dots$) which can be determined by calculating the Berry curvature $\mathbf{\Omega}_{\mathbf{k}}$ ($\oint d\mathbf{s} \cdot \mathbf{\Omega}_{\mathbf{k}} = 2\pi\eta$, $\mathbf{\Omega}_{\mathbf{k}} = i\nabla \times \langle u_{\mathbf{k}} | \nabla_{\mathbf{k}} u_{\mathbf{k}} \rangle$, where $|u_{\mathbf{k}}\rangle$ is the Bloch wave function) [2, 3]. The electronic dispersion and transport phenomena associated with WSMs have been explored by a number of experimental [4–9] and theoretical studies [10–16]. The distinct topology of the WSM leads to various unique electronic and transport properties such as, Fermi arc surface states connecting a pair of Weyl nodes, Adler–Bell–Jackiw (ABJ) anomaly and negative magnetoresistance [17–21]. Besides, WSMs also exhibit superconducting phases [22–25], and the chiral Hall effect [26, 27]. The WSM phase was first observed in the candidate material TaAs [28–30] and later NbAs, TaP and NbP [31, 32].

An important aspect of the study of WSM materials is their magnetic ordering. WSMs lack spontaneous magnetic ordering originating from the Heisenberg interaction. However magnetic interactions may be generated between magnetic impurities through an indirect exchange coupling mechanism namely the Ruderman-Kittel-Kasuya-Yoshida (RKKY) interaction. For a system with magnetic impurities, the coupling is generated from the Heisenberg exchange interaction between the impurities and the conduction electrons near the Fermi level, which can be modeled by the second-order perturbation theory.

Several theoretical works have been made to address the long-range RKKY type magnetic interaction in WSMs. A study of the RKKY interaction for both the TRS breaking and IR breaking WSMs has been done by Ref. [33], but, in the absence of any dispersion tilt. This study reveals the presence of only the conventional long-range Heisenberg type coupling. In the presence of tilt and for the TRS-breaking WSMs the RKKY interaction between the magnetic impurities in WSM has been studied in Ref. [34]. The work assumes the presence of real-spin-momentum locking and considers only the special case where the tilt direction is fixed along the vector connecting the two Weyl nodes. However, most of the WSMs experimentally studied so far are found to be IR-breaking. Besides, these WSM systems lack real spin-momentum locking and instead exhibit pseudo-spin momentum locking, as described by most of the minimal energy Hamiltonians of WSM in the literature [28, 29, 31].

In the conventional RKKY interactions, e.g., in diluted magnetic semiconductors [35–37], in topological insulators [38, 39], the RKKY interaction is spatially isotropic and is a function only of the separation distance between the magnetic impurities. By contrast, in this paper we will consider the RKKY interactions in both the TRS and IR breaking WSMs where the isotropy is broken by the presence of tilt in the energy dispersion. Thus, in our system there are three directions under consideration: the direction of the tilt, the separation vector between two impurities and the vector joining the two Weyl nodes. We will explore the directional dependence of the RKKY interaction as a result of the interplay of these three special directions, and utilize the corresponding degrees of directional freedom to modulate the RKKY coupling and switch its sign i.e., from ferromagnetic to anti-ferromagnetic coupling and vice-versa.

In this manuscript, we will investigate the effect of dispersion tilt on the RKKY coupling for two special cases: (1) when time-reversal symmetry (TRS) is broken but inversion symmetry (IR) is intact, i.e., when a pair of WPs are separated in momentum space (\mathbf{Q}) but the nodes appear at the same energy and (2) when IR is broken but TRS is intact i.e. when WPs are separated along energy axis (ϵ_0). In addition, we will consider the contributions to the RKKY interaction which originate from the scattering between any two energy states within a particular band, namely intra-band scattering, as well as scattering between different bands with either the same or opposite chiralities, namely inter-band scattering.

II. METHOD

The Hamiltonian for a tilted WSM around a pair of Weyl nodes is [33, 40–43],

$$H_0 = \eta \hbar v_F \boldsymbol{\tau} \cdot (\mathbf{k} - \eta \mathbf{Q}) + \hbar \mathbf{w}_\eta \cdot (\mathbf{k} - \eta \mathbf{Q}) \tau_0 + \eta \tau_0 \epsilon_0, \quad (1)$$

where, $\eta = \pm 1$ indicates the chirality of the Weyl nodes in the two valleys, $2\mathbf{Q}$ is the separation between them in the momentum space and $2\epsilon_0$ is the separation along the energy axis, $\boldsymbol{\tau}$ is the Pauli vector acting on the chirality space and \mathbf{w}_η is the tilt vector for the Weyl nodes with chirality η . The tilt serves as an additional anisotropy term in the

Hamiltonian [44]. The corresponding energy dispersion is as follows, $\epsilon_{\mathbf{k},\eta} = \eta v_F |\mathbf{k} - \eta \mathbf{Q}| + \mathbf{w}_\eta \cdot (\mathbf{k} - \eta \mathbf{Q}) + \eta \epsilon_0$.

To calculate the RKKY interaction, we consider two impurities with magnetic moments \mathbf{S}_1 and \mathbf{S}_2 and situated at \mathbf{R}_1 and \mathbf{R}_2 . The s-d interaction between the conduction electrons and the two impurities can be regarded as a perturbation term, $H'(\mathbf{r}) = J \sum_{i=1,2} \mathbf{S}_i \cdot \boldsymbol{\sigma} \delta(\mathbf{r} - \mathbf{R}_i)$, where \mathbf{r} represents position coordinate and the $\boldsymbol{\sigma}$ corresponds to Pauli vector representing real spin degrees of freedom. The RKKY interaction can be obtained by using the second-order perturbation theory [45]. The second order energy correction due to the above perturbation is,

$$\epsilon^{(2)} = \sum_{\mathbf{k}'\eta'(\neq\mathbf{k}\eta)} \frac{|\langle \mathbf{k}\eta | H'(\mathbf{r}) | \mathbf{k}'\eta' \rangle|^2}{\epsilon_{\mathbf{k}'\eta'} - \epsilon_{\mathbf{k}\eta}} (f_{\mathbf{k}'\eta'} - f_{\mathbf{k}\eta}), \quad (2)$$

where $f_{\mathbf{k}'\eta'}$ and $f_{\mathbf{k}\eta}$ are the Fermi functions corresponding to the two valleys η and η' . While carrying out the summation above, we separate the contribution from the intra-valley transition, i.e., transition between two states within a valley with a particular chirality ($\eta = \eta'$) and the inter-valley transition between two valleys with opposite chiralities ($\eta \neq \eta'$). With this we rewrite the above term as follows,

$$\epsilon^{(2)} = 2 (\mathbf{S}_1 \cdot \mathbf{S}_2) F(\mathbf{R}), \quad (3)$$

where, $\mathbf{R} = |\mathbf{R}| = |\mathbf{R}_1 - \mathbf{R}_2|$ and $F(\mathbf{R})$ is typically known to be the RKKY range function which is given by,

$$F(\mathbf{R}) = \sum_{\eta} F_{\text{intra}}^{\eta}(\mathbf{R}) + \sum_{\eta} e^{i(\eta 2\mathbf{Q} \cdot \mathbf{R})} F_{\text{inter}}^{\eta, -\eta}(\mathbf{R}). \quad (4)$$

In the above, we separate out the intra and inter-valley contributions. The intra-valley contribution in the above can be given as (after changing $\sum_{\mathbf{k}'\eta'(\neq\mathbf{k}\eta)} \rightarrow \int d\mathbf{k} \int d\mathbf{k}'$),

$$F_{\text{intra}}^{\eta}(\mathbf{R}) = \left(\frac{1}{\hbar v_F} \right) \text{Re} \int_{k=0}^{k_{F\eta}} d\mathbf{k} \int_{k'=k_{F\eta}}^{\infty} d\mathbf{k}' \frac{e^{i(\mathbf{k}'-\mathbf{k}) \cdot \mathbf{R}}}{(k' - k) + \frac{\mathbf{w}_\eta}{v_F} \cdot (\mathbf{k}' - \mathbf{k})}, \quad (5)$$

where $k = |\mathbf{k}|$, $k' = |\mathbf{k}'|$ and $k_{F\eta}$ is the Fermi wave vector corresponding to a valley with chirality η and is defined by, $\epsilon_F = \hbar v_F k_{F\eta} + \eta \epsilon_0$. Similarly, the inter-valley contribution can be expressed as,

$$F_{\text{inter}}^{\eta, -\eta}(\mathbf{R}) = \left(\frac{1}{\hbar v_F} \right) \text{Re} \int_{k=0}^{k_{F\eta}} d\mathbf{k} \int_{k'=k_{F,-\eta}}^{\infty} d\mathbf{k}' \frac{e^{i(\mathbf{k}'-\mathbf{k}) \cdot \mathbf{R}}}{(k' - k) + \left(\frac{\mathbf{w}_{-\eta}}{v_F} \cdot \mathbf{k}' - \frac{\mathbf{w}_\eta}{v_F} \cdot \mathbf{k} \right) - \eta 2\epsilon_0}. \quad (6)$$

We calculate the integrations in above two functions (Eqs. (5) and (6)) for different types of WSMs. In usual RKKY calculation the oscillatory decaying range function originates from the singularity (poles) in the denominator. In the absence of tilt ($\mathbf{w}_\eta = 0$) the pole occurs at $k' = k$ in Eq. (5) and $k' = k + \eta 2\epsilon_0$ in Eq. (6). However, in the presence of a finite tilt, the poles occur at $\mathbf{k}' = \mathbf{k}$, i.e., the solution for the poles depends on the directions of the wave vectors. In this case, it is no longer possible to solve the integral analytically when the tilt \mathbf{w} and the separation vector \mathbf{R} are aligned along with arbitrary directions. The analytical expression for the integral can only be obtained by considering the small tilt limit and expanding the expressions in the integrals of Eqs. (5) and (6) up to the second-order in tilt parameter. Finally, we consider two types of tilt in our analysis, parallel tilt i.e., when $\mathbf{w}_\eta = \mathbf{w}$ for a pair of Weyl nodes and opposite tilt i.e., when $\mathbf{w}_\eta = \eta \mathbf{w}$. For each type of tilt, we calculate the effects of tilt for both the TRS breaking and IR breaking cases.

III. SMALL TILT LIMIT ($|\mathbf{w}_\eta|/v_F \ll 1$)

In the small tilt limit, we perform a Taylor expansion of the intra-valley range function to the second-order in tilt (see Supplemental Information for the detailed calculations). The intra-valley range function in that case can be expressed as,

$$F_{\text{intra}}^{\eta}(\mathbf{R}) = \sum_{m=0}^2 \left(\frac{\mathbf{w}_\eta}{v_F} \cdot \frac{\partial}{\partial \mathbf{R}} \right)^m \chi^{(m)}(\mathbf{R}), \quad (7)$$

where,

$$\chi^{(m)}(\mathbf{R}) = \left(\frac{1}{\hbar v_F} \right) \text{Re}(-i)^m \int_{k=0}^{k_{F\eta}} d\mathbf{k} \int_{k'=k_{F\eta}}^{\infty} d\mathbf{k}' \frac{e^{i(\mathbf{k}'-\mathbf{k})\cdot\mathbf{R}}}{(k'-k)^{m+1}}. \quad (8)$$

Performing a similar expansion of the inter-valley range function,

$$F_{\text{inter}}^{\eta,-\eta}(\mathbf{R}) = \sum_{m=0}^2 \zeta^{(m,\eta,-\eta)}(\mathbf{R}), \quad (9)$$

where,

$$\zeta^{(m,\eta,-\eta)}(\mathbf{R}) = \text{Re} \int_{k=0}^{k_{F\eta}} d\mathbf{k} \int_{k'=k_{F,-\eta}}^{\infty} d\mathbf{k}' \frac{\hbar^m (\mathbf{w}_\eta \cdot \mathbf{k}' - \mathbf{w}_{-\eta} \cdot \mathbf{k})^m e^{i(\mathbf{k}'-\mathbf{k})\cdot\mathbf{R}}}{(\hbar v_F (k' - k) \mp 2\epsilon_0)^{m+1}}. \quad (10)$$

One can immediately see, the first-order term ($m = 1$) in Eqs. (7 and 10) is linearly dependent on the wave-vector and as result would become zero after integration over the angular part (see Supplemental materials). So, the total RKKY range function (omitting the 1st order in $|\mathbf{w}|$ -terms) is,

$$F(\mathbf{R}) = \sum_{m=\{0,2\}} \sum_{\eta} \left(\frac{\mathbf{w}_\eta}{v_F} \cdot \frac{\partial}{\partial \mathbf{R}} \right)^m \chi^{(m)}(\mathbf{R}) + \sum_{m=\{0,2\}} \sum_{\eta} \zeta^{(m,\eta,-\eta)}(\mathbf{R}). \quad (11)$$

Next, we consider two types of WSMS: (a) when TRS is broken, i.e., the Weyl nodes are separated in k -space with band touching points at the same energy ($\epsilon_0 = 0$) and (b) when IR is broken, where the nodes are separated along energy axis ($\mathbf{Q} = 0$). For each type, we consider both cases where the tilt vectors at the two Weyl nodes are parallel ($\mathbf{w}_\eta = \mathbf{w}$) and when they are chiral or opposite to one another ($\mathbf{w}_\eta = \eta \mathbf{w}$). It turns out (as will be shown later) while the RKKY range functions are strongly dependent on the magnitude of tilt, the tilt configuration in the two Weyl nodes (either parallel or chiral) does not play such a significant role in determining the RKKY coupling. Hence, we will only present the results for the parallel tilt case in the main manuscript, while similar results for the chiral tilt case are presented in the Supplemental section. On the other hand, the type of symmetry-breaking would significantly affect the RKKY coupling and would be presented separately in the main manuscript.

A. Broken TRS ($\epsilon_0 = 0$ and $\mathbf{Q} \neq 0$)

We first consider the TRS breaking case, for which the corresponding Hamiltonian from Eq. (1) is, $H_0 = \eta v_F \boldsymbol{\tau} \cdot (\mathbf{k} - \eta \mathbf{Q}) + \mathbf{w}_\eta \cdot (\mathbf{k} - \eta \mathbf{Q}) \tau_0$. Since the Fermi wave vector is the same for both Weyl nodes, the integration limits in Eq. (5) and (6) simplify to, $\int_{k=0}^{k_F} d\mathbf{k} \int_{k'=k_F}^{\infty} d\mathbf{k}'$ where $k_F = \epsilon_F / \hbar v_F$. For the special case of $\mathbf{w} \parallel \hat{z}$ and in the limit of small tilt, we can derive the analytical expression of the total range function. Denoting $\zeta^{(0,\eta,-\eta)}(\mathbf{R}) = \chi^{(0,\eta)}(\mathbf{R})$ and $\zeta^{(2,\eta,-\eta)}(\mathbf{R}) = -\left(\frac{\mathbf{w}}{v_F} \cdot \frac{\partial}{\partial \mathbf{R}} \right)^2 \chi^{(2,\eta)}(\mathbf{R})$ in Eqs. (4, 7, 9), we obtain the following

$$F(\mathbf{R}) = 2(1 + \cos(2\mathbf{Q} \cdot \mathbf{R})) \left(\chi^{(0,\eta)}(\mathbf{R}) - \left(\frac{\mathbf{w}}{v_F} \cdot \frac{\partial}{\partial \mathbf{R}} \right)^2 \chi^{(2,\eta)}(\mathbf{R}) \right), \quad (12)$$

where,

$$\chi^{(0,\eta)}(\mathbf{R}) = \frac{4\pi^3 \left((3 - 6k_F^2 R^2) \cos(2k_F R) + 6k_F R \sin(2k_F R) - 3 \right)}{3R^5}, \quad (13)$$

$$\chi^{(2,\eta)}(\mathbf{R}) = \frac{4\pi^3 \left(-3(4k_F^2 R^2 + 1) + 3(2k_F^2 R^2 + 1) \cos(2k_F R) + 6k_F R \sin(2k_F R) \right)}{3R^3}, \quad (14)$$

$$\begin{aligned} \left(\frac{|\mathbf{w}|}{v_F} \frac{\partial}{\partial R_z} \right)^2 \chi^{(2,\eta)}(\mathbf{R}) &= \left(\frac{|\mathbf{w}|}{v_F} \right)^2 \frac{2\pi^3 \left(-3 \cos^2(\theta) (4k_F^2 R^2 + 5) + k_F R \sin(2k_F R) (\cos(2\theta) (2k_F^2 R^2 + 15) - 2k_F^2 R^2 + 9) \right)}{R^5} \\ &+ \left(\frac{|\mathbf{w}|}{v_F} \right)^2 \frac{2\pi^3 \left(4k_F^2 R^2 + \cos(2k_F R) (2k_F^2 R^2 + \cos^2(\theta) (-8k_F^4 R^4 - 18k_F^2 R^2 + 15) - 3) + 3 \right)}{R^5}. \end{aligned} \quad (15)$$

In the limit of large R , the functions $\chi^{(0,\eta)}(\mathbf{R}) \propto \cos(2k_F R)/R^3$ and $(\partial/\partial R)^2 \chi^{(2,\eta)}(\mathbf{R}) \propto 2/R - \cos(2k_F R)/R$. The second term in Eq.(12) provides two types of coupling: (i) the tilt direction (\mathbf{w}) with the impurity separation direction (\mathbf{R}), and (ii) the coupling between \mathbf{Q} and \mathbf{R} from the $\cos(2\mathbf{Q} \cdot \mathbf{R})$ term. The $\cos(2\mathbf{Q} \cdot \mathbf{R})$ term has already been studied by the Refs. [34]. However the effect of that term would be negligible in two special scenarios: (i) in the limit of large Weyl node separation ($|\mathbf{Q}| \gg k_F$), in which case the summation over all the impurities i.e. summation over all \mathbf{R} becomes negligibly small because of the very high oscillation of the cosine function and as a consequence the term does not result in any significant directional dependence; (ii) in the limit of small Weyl node separation ($|\mathbf{Q}| \ll k_F$) in which case the envelope function varies slowly over R and as a consequence the range function is mostly determined by the usual RKKY function within the envelope.

The above results show that the RKKY range function exhibits a distinct anisotropy in the presence of tilt vector \mathbf{w} . This is unlike the RKKY range function in graphene, Rashba or other spintronics systems, where the RKKY is isotropic and dependent only on the distance between the impurities (R). We will now analyze the anisotropy of the RKKY range function numerically.

Numerical results for broken TRS: In our numerical calculations, we set $\mathbf{R} = R(\sin(\theta) \cos(\phi) \hat{x} + \sin(\theta) \sin(\phi) \hat{y} + \cos(\theta) \hat{z})$. In a WSM the x , y , z -axes may coincide with the crystal axes. The integrations in Eqs. (7) and (9) are performed numerically for $\epsilon_0 = 0$. In Fig 1(a), we plot the total RKKY range function $F(\mathbf{R})$ while varying R for the special case of $\mathbf{w} \parallel \mathbf{Q} \parallel \mathbf{R} \parallel \hat{z}$. At the small R limit, the envelope function has a $1/R^3$ dependence, as can be seen from the inset. In this limit, the RKKY function has a similar dependence compared to the non-tilted WSMs. However for a sufficiently large value of R and in the presence of tilt the envelope function approaches $1/R$ dependence matching our analytical results. Next, in Fig. 1(b) and (c), we plot the angular dependence of the range function $F(\mathbf{R})$. In Fig. 1(b), we show the angular dependence of $F(\mathbf{R})$ by varying the angle (θ) between \mathbf{w} and \mathbf{R} while fixing the tilt direction to be $\mathbf{w} \parallel \hat{z}$. In Fig. 1(c), we plot the angular dependence of $F(\mathbf{R})$ by varying the angle (ϕ) between \mathbf{R} and x -axis while fixing the tilt vector $\mathbf{w} \parallel (\hat{x} + \hat{y})$, i.e., it lies in the x - y plane. For both cases, the range function oscillates with the angle between tilt and the separation vector \mathbf{R} . In Fig 1(d), we plot the angular dependence of $F(\mathbf{R})$ as a function of both with polar angle (θ) and azimuthal angle (ϕ) while fixing the tilt vector $\mathbf{w} \parallel (\hat{x} + \hat{y})$. There is significant variation in the range function with both θ and ϕ , i.e., showing a strong directional dependence on the separation vector \mathbf{R} .

B. Broken IR ($\mathbf{Q} = 0$ and $\epsilon_0 \neq 0$)

Next, we investigate the WSM systems where the inversion symmetry is broken. The corresponding Hamiltonian can be obtained by letting $\mathbf{Q} = 0$ in the Hamiltonian of Eq. (1), i.e., $H_0 = \eta v_F \boldsymbol{\tau} \cdot \mathbf{k} + \mathbf{w}_\eta \cdot \mathbf{k} \tau_0 + \eta \epsilon_0 \tau_0$. The Dirac nodes in this case are separated along the energy axis. In this case, the Fermi surface has different sizes for the two different valleys, i.e., $k_{F\eta} \neq k_{F\bar{\eta}}$ and as a consequence, the intra and inter-valley range functions are different from that of the TRS-breaking case. Assuming parallel tilt vectors for both the valleys, i.e., $\mathbf{w}_\eta = \mathbf{w}$ and using the Eq. (7) and Eq. (9); the expression for the total range function is given as follows,

$$\begin{aligned} F(\mathbf{R}) &= \left\{ \sum_\eta \chi_{IR}^{(0,\eta)}(\mathbf{R}) - \sum_\eta \left(\frac{\mathbf{w}}{v_F} \cdot \frac{\partial}{\partial \mathbf{R}} \right)^2 \chi_{IR}^{(2,\eta)}(\mathbf{R}) \right\} \\ &+ \left\{ \sum_\eta \left[\zeta_{IR}^{(0)}(\eta, -\eta, \mathbf{R}) - \left(\frac{\mathbf{w}}{v_F} \cdot \frac{\partial}{\partial \mathbf{R}} \right)^2 \zeta_{IR}^{(2)}(\eta, -\eta, \mathbf{R}) \right] \right\}. \end{aligned} \quad (16)$$

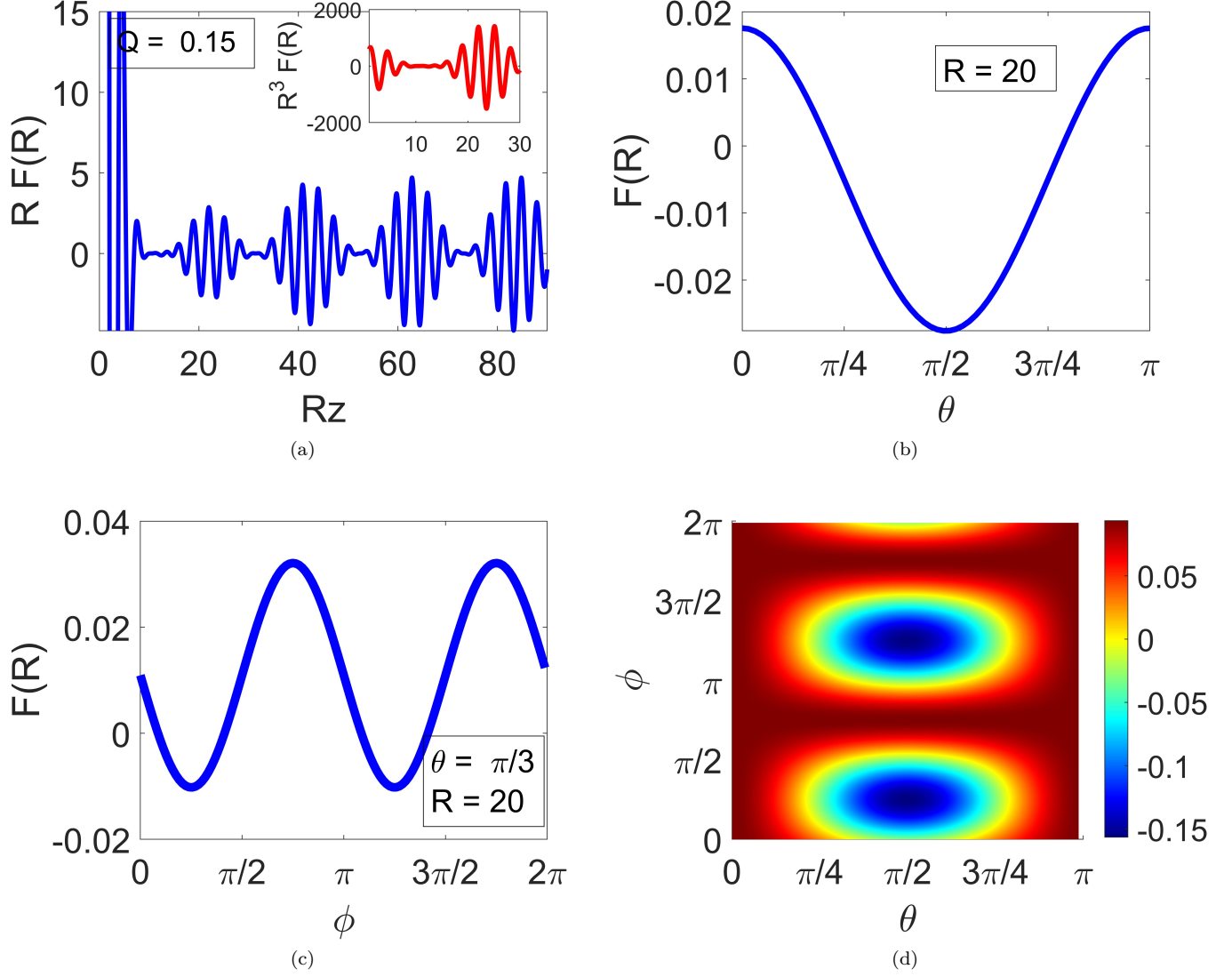


FIG. 1: WSMs with broken TRS: $|\mathbf{w}|/v_F = 0.05$ (a) $R F(\mathbf{R})$ is plotted as a function of R , for the tilt $\mathbf{w} \parallel \hat{z}$. In the inset, $R^3 F(\mathbf{R})$ is plotted as a function of R . (b) $F(\mathbf{R})$ is plotted as a function of θ for the tilt vector $\mathbf{w} \parallel \hat{z}$. (c) $F(\mathbf{R})$ is plotted as a function of ϕ and for the tilt vector $\mathbf{w} \parallel \hat{x} + \hat{y}$ (d) $F(\mathbf{R})$ is plotted as a function of both polar angle θ and azimuthal angle ϕ . For (b)-(d), we set $k_F R = 20$.

In the above, the intra-valley and the inter-valley contributions at zero tilt are given explicitly as follows,

$$\begin{aligned} \sum_{\eta} \chi_{IR}^{(0,\eta)}(\mathbf{R}) = & \frac{4\pi^3 \left((3 - 6R^2(q_0 - k_F)^2) \cos(2R(k_F - q_0)) + (3 - 6R^2(q_0 + k_F)^2) \cos(2R(q_0 + k_F)) \right)}{3R^5} \\ & + \frac{4\pi^3 (6R(k_F - q_0) \sin(2R(k_F - q_0)) + 6R(q_0 + k_F) \sin(2R(q_0 + k_F)) - 6)}{3R^5}, \end{aligned} \quad (17)$$

$$\begin{aligned}
\sum_{\eta} \zeta_{IR}^{(0)}(\eta, -\eta, \mathbf{R}) &= \frac{4\pi^3 (-4q_0 \mathbf{R} (4\mathbf{R}^2 (2q_0^2 + 3k_F^2) + 3) \sin(2q_0 \mathbf{R}))}{3\mathbf{R}^5} \\
&+ \frac{4\pi^3 (3 (1 - 2\mathbf{R}^2 (3q_0^2 - 4q_0 k_F + k_F^2)) \cos(2\mathbf{R}(k_F - 2q_0)))}{3\mathbf{R}^5} \\
&+ \frac{4\pi^3 (-3 (2\mathbf{R}^2 (q_0 + k_F)(3q_0 + k_F) - 1) \cos(2\mathbf{R}(2q_0 + k_F)))}{3\mathbf{R}^5} \\
&+ \frac{4\pi^3 (6\mathbf{R}(k_F - 2q_0) \sin(2\mathbf{R}(k_F - 2q_0)) + 6\mathbf{R}(2q_0 + k_F) \sin(2\mathbf{R}(2q_0 + k_F)) - 6 \cos(2q_0 \mathbf{R}))}{3\mathbf{R}^5}, \quad (18)
\end{aligned}$$

and, the intra-valley and the inter-valley contributions to the second order in the tilt parameter can be expressed as follows,

$$\chi_{IR}^{(2,\eta)}(\mathbf{R}) = \frac{4\pi^3 (-4\mathbf{R}^2 (q_F - \eta q_0)^2 + (2\mathbf{R}^2 (q_F - \eta q_0)^2 + 1) \cos(2\mathbf{R}(q_F - \eta q_0)) + 2\mathbf{R}(q_F - \eta q_0) \sin(2\mathbf{R}(q_F - \eta q_0)) - 1)}{\mathbf{R}^3}, \quad (19)$$

$$\begin{aligned}
\zeta_{IR}^{(2)}(\eta, -\eta, \mathbf{R}) &= \frac{4\pi^3 (2\mathbf{R} (3\eta q_0 - 2\mathbf{R}^2 (k_F - 4\eta q_0)(k_F - \eta q_0)^2) \sin(2\eta q_0 \mathbf{R}) - 3 (4\mathbf{R}^2 (k_F - \eta q_0)^2 + 1) \cos(2\eta q_0 \mathbf{R}))}{3\mathbf{R}^3} \\
&+ \frac{4\pi^3 (3 (2\mathbf{R}^2 (k_F - \eta q_0)(k_F - 3\eta q_0) + 1) \cos(2\mathbf{R}(k_F - 2\eta q_0)) + 6k_F \mathbf{R} \sin(2\mathbf{R}(k_F - 2\eta q_0)))}{3\mathbf{R}^3}, \quad (20)
\end{aligned}$$

where, $q_0 = \epsilon_0/\hbar v_F$. The full expression of all the second-order derivative functions are given in the Supplemental. Similar to the TRS case the $\chi^{(0,\eta)}(\mathbf{R})$ and $\zeta^{(0)}(\eta, -\eta, \mathbf{R})$ functions have a $1/\mathbf{R}^3$ dependence while $\chi^{(2,\eta)}(\mathbf{R})$ varies with $1/\mathbf{R}$. Specifically at large R , the $1/\mathbf{R}$ dependence dominates and the total range function varies as,

$$\begin{aligned}
F(\mathbf{R}) &\propto \frac{16\pi^3 |\mathbf{w}|^2}{\mathbf{R}} \\
&(-4k_F^2 q_0^2 \cos(2q_0 \mathbf{R}) + 2k_F^2 (k_F^2 - q_0^2) \cos(2k_F \mathbf{R}) + (k_F - q_0)^4 \cos(2\mathbf{R}(k_F - q_0)) + (k_F + q_0)^4 \cos(2\mathbf{R}(k_F + q_0))). \quad (21)
\end{aligned}$$

Numerical results for broken IR: The integrations in Eqs. (7) and (9) are performed numerically for $\mathbf{Q} = \mathbf{0}$. In Fig 2(a), we plot the total RKKY range function $\mathbf{R}F(\mathbf{R})$ while varying \mathbf{R} for the special case of $\mathbf{w} \parallel \mathbf{R} \parallel \hat{z}$. At the small \mathbf{R} limit, the envelope function varies with $1/\mathbf{R}^3$ as can be seen from the inset. In this limit, the RKKY function has a similar dependence as that of non-tilted WSMs. However for a sufficiently large value of \mathbf{R} and in the presence of tilt the envelope function has a $1/\mathbf{R}$ dependence. In Fig. 2(b), we show that the angular dependence of $F(\mathbf{R})$ by varying the angle between \mathbf{w} and \mathbf{R} while fixing the tilt direction $\mathbf{w} \parallel \hat{z}$. In Fig 2(c), we plot the angular dependence of $F(\mathbf{R})$ by varying the angle between \mathbf{R} and x -axis while fixing the tilt vector $\mathbf{w} \parallel (\hat{x} + \hat{y})$ i.e. tilt vector lies in the x - y plane. In Fig 2(d), we show the angular dependence of $F(\mathbf{R})$ as a function of both the polar angle (θ) and azimuthal angle (ϕ) while fixing the tilt vector $\mathbf{w} \parallel (\hat{x} + \hat{y})$. For Fig 2(a)-(d) we choose $q_0/k_F = 0.15$.

Several observations can be made immediately by comparing Fig. 2 and Fig. 1. The separation between the nodes i.e. $|\mathbf{Q}|$ for TRS breaking and q_0 for the IR breaking WSMs respectively produce similar envelope function in both Fig. 1(a) and Fig. 2(a). The difference in magnitude between TRS and IR-breaking system is not very significant. For both the TRS and IR-breaking WSM systems, it is possible to switch the RKKY-induced exchange coupling from ferromagnetic (i.e., $F(\mathbf{R}) < 0$) to anti-ferromagnetic (i.e., $F(\mathbf{R}) > 0$) coupling by varying both the angles θ and ϕ associated with the separation vector \mathbf{R} , as shown in Figs. 1(d) and 2(d).

Note that for the TRS breaking case, the directional dependence of the range function arises due to the $\cos(2\mathbf{Q} \cdot \mathbf{R})$ term as can be seen from Eq. (12). This term produces an extra oscillation with respect to the angular variation on top of the intra-valley range function [43]. However the effect of this term vanishes for the special case when $\mathbf{Q} \perp \mathbf{R}$, i.e., when the separation between nodes is perpendicular to spatial vector between impurities. For the case of IR breaking WSMs, the analytical expression of the envelope function cannot be factored out analytically, and thus we cannot similarly find a spatial direction where the oscillatory dependence on the angular direction vanishes.

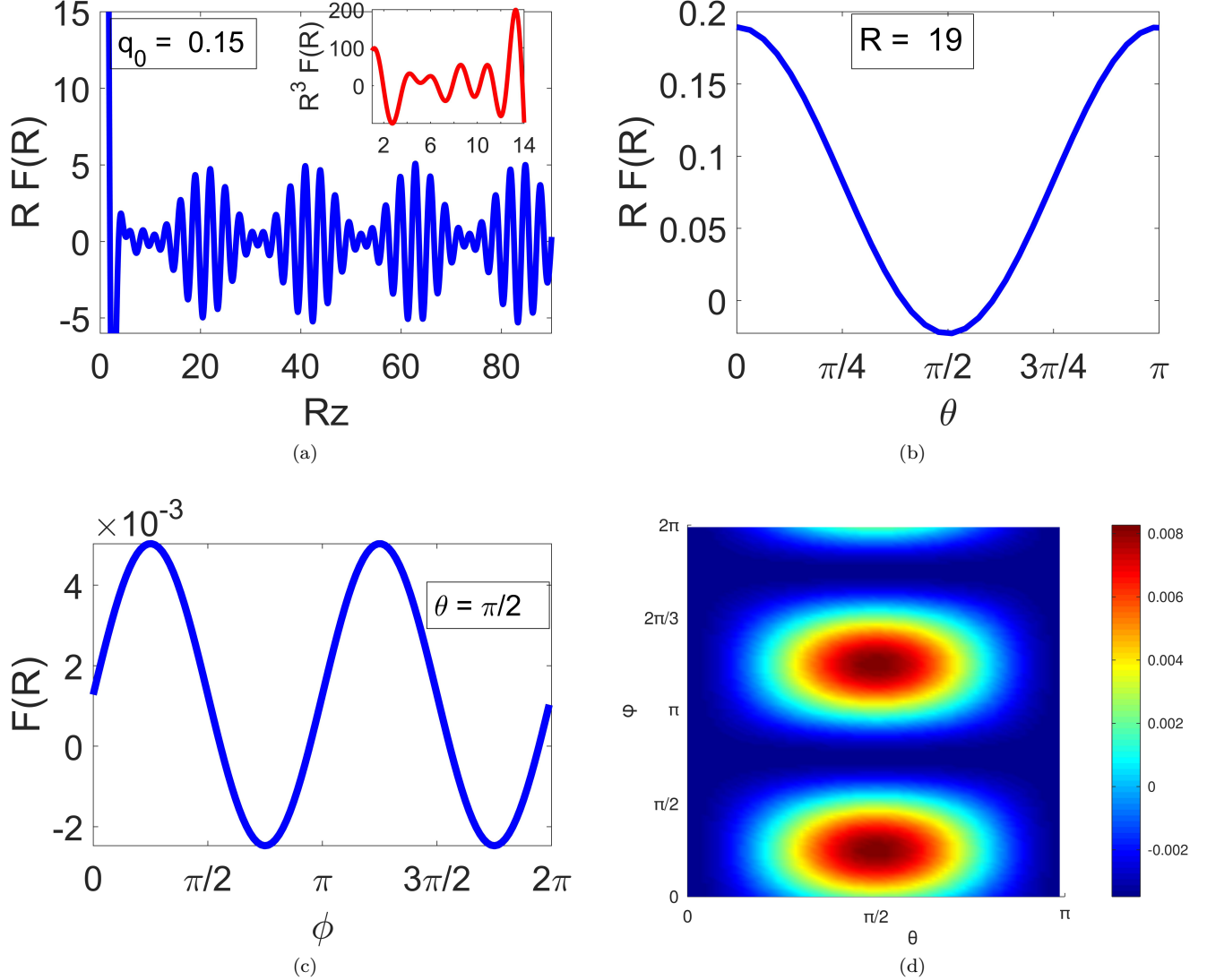


FIG. 2: IR breaking WSM: $|\mathbf{w}|/v_F = 0.05$, (a) Plot of $RF(R)$ and the inset is the small R limit, for the tilt $\mathbf{w} \parallel \hat{z}$ (b) Range function vs. θ for the tilt, $\mathbf{w} \parallel \hat{z}$ (c) Range function vs. ϕ and for tilt, $\mathbf{w} \parallel \hat{x} + \hat{y}$ (d) Range function vs. both polar angle θ and azimuthal angle ϕ . For (b)-(d), we choose $k_F R = 20$.

C. Opposite Tilt ($\mathbf{w}_\eta = \eta \mathbf{w}$)

We also calculate the RKKY range function for the case where the dispersion cones are tilted in opposite directions for Weyl nodes of opposite chirality (i.e. $\mathbf{w}_\eta = \eta \mathbf{w}$). In this case, the range function differs from the parallel tilt case in the second-order in terms of the tilt parameter. **TRS broken** ($\epsilon_0 = 0$): The total range function is now given by,

$$F(\mathbf{R}) = 2(1 + \cos(2\mathbf{Q} \cdot \mathbf{R})) \left(\chi^{(0,\eta)}(\mathbf{R}) + \chi^{(2,\eta)}(\mathbf{R}) \right), \quad (22)$$

where,

$$\chi^{(2,\eta)}(\mathbf{R}) = -\text{Re} \int_{k=0}^{k_F \eta} d\mathbf{k} \int_{k'=0}^{\infty} d\mathbf{k}' \frac{(\mathbf{w} \cdot (\mathbf{k}' + \mathbf{k}))^2 e^{i(\mathbf{k}' - \mathbf{k}) \cdot \mathbf{R}}}{(\hbar v_F (k' - k))^3}. \quad (23)$$

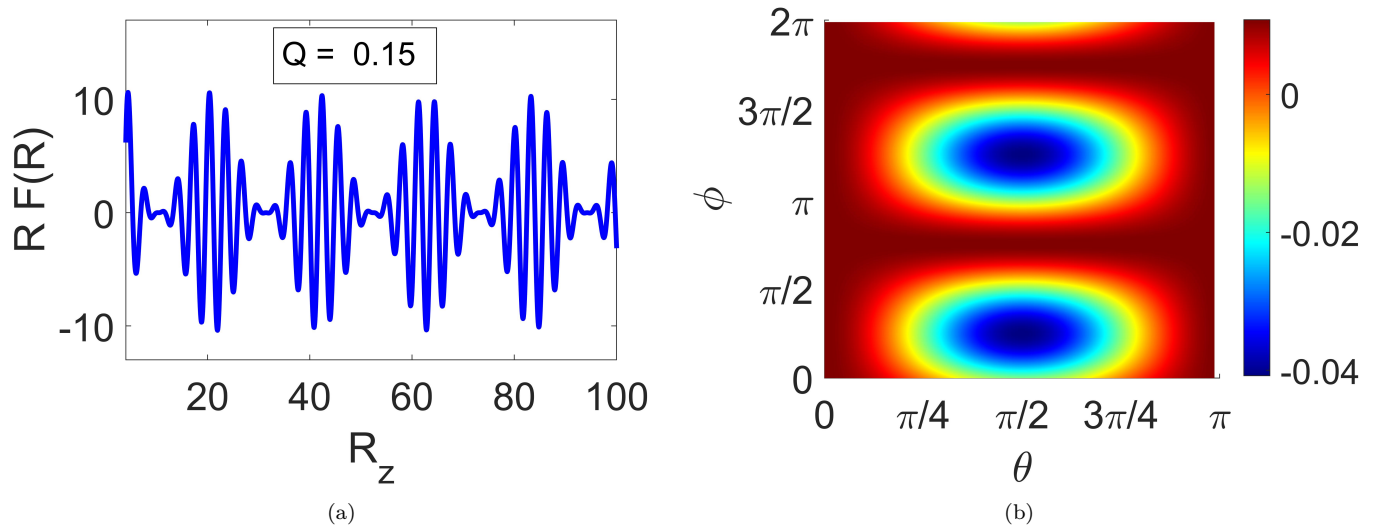


FIG. 3: TRS breaking WSM with the tilt $\mathbf{w} \parallel \hat{z}$ and $|\mathbf{w}|/v_F = 0.05$: (a) Plot of $R F(\mathbf{R})$ as a function of R which is along the z -direction, (b) Contour plot of the range function $F(\mathbf{R})$ as a function of both polar angle θ and azimuthal angle ϕ with $k_F R = 20$.

We rewrite the above equation as,

$$\begin{aligned}
\chi^{(2,\eta)}(\mathbf{R}) = & \mathbf{Re} \left(\left(\frac{\mathbf{w}}{v_F} \cdot \frac{\partial}{\partial \mathbf{R}} \right)^2 \int_{k=0}^{k_{F\eta}} d\mathbf{k} e^{-i\mathbf{k} \cdot \mathbf{R}} \right) \int_{k'=0}^{\infty} dk' \frac{e^{i\mathbf{k}' \cdot \mathbf{R}}}{(\hbar v_F (k' - k))^3} \\
& + \mathbf{Re} \int_{k=0}^{k_{F\eta}} d\mathbf{k} e^{-i\mathbf{k} \cdot \mathbf{R}} \left[\left(\frac{\mathbf{w}}{v_F} \cdot \frac{\partial}{\partial \mathbf{R}} \right)^2 \int_{k'=0}^{\infty} dk' \frac{e^{i\mathbf{k}' \cdot \mathbf{R}}}{(\hbar v_F (k' - k))^3} \right] \\
& + 2\mathbf{Re} \left[\left(\frac{\mathbf{w}}{v_F} \cdot \frac{\partial}{\partial \mathbf{R}} \right) \int_{k=0}^{k_{F\eta}} d\mathbf{k} e^{-i\mathbf{k} \cdot \mathbf{R}} \right] \left[\left(\frac{\mathbf{w}}{v_F} \cdot \frac{\partial}{\partial \mathbf{R}} \right) \int_{k'=0}^{\infty} dk' \frac{e^{i\mathbf{k}' \cdot \mathbf{R}}}{(\hbar v_F (k' - k))^3} \right]. \quad (24)
\end{aligned}$$

As before, the full expressions of the above are given in the supplemental due to the size of the expressions. In Fig 3(a), we plot the total RKKY range function $F(\mathbf{R})$ while varying R for the special case of $\mathbf{w} \parallel \mathbf{Q} \parallel \mathbf{R} \parallel \hat{z}$. In Fig. 3(b), we plot the angular dependence of $F(\mathbf{R})$ as a function of both with polar angle (θ) and azimuthal angle (ϕ) while we keep $\mathbf{w} \parallel \hat{z}$. Similar to the parallel tilt case, range function varies with the changes in θ and ϕ , i.e., showing a strong directional dependence on the separation vector \mathbf{R} .

Finite tilt limit: Thus far, we have considered the analytical expression of the RKKY range function in the small-tilt limit. We also analyze the RKKY range function numerically for any arbitrary tilt value. In doing so, we consider the general expressions in Eqs. (4-9), assume parallel tilt vector for all Weyl nodes and set the tilt as $\mathbf{w} \parallel \hat{z}$. The corresponding plots for these numerical calculations are given in the supplemental. Generally, in the small tilt limit the RKKY function is linearly dependent on tilt matching our analytical result. However, at the large tilt limit, the variation of the RKKY range function with the tilt magnitude diverges from the analytical results, and assumes a non-linear variation.

IV. DISCUSSION

We explicitly study the effect of tilted energy dispersion on the RKKY coupling strength for two types of WSMs, namely, the TRS-broken and IR-broken. The direction of the tilt can be determined from the band structure and can vary with the crystal axis in different materials. We fix the direction of tilt and analyze the RKKY range function with varying magnitude and direction of \mathbf{R} . The range function in the absence of tilt varies as $1/R^3$ for both the TRS and IR breaking system. Interestingly, however, in the presence of tilt, the the total range function varies as $1/R$ in the limit of large R . This means that the dispersion tilt can have a significant effect on the overall RKKY effect in

WSMs even though the tilt-dependent term is only second-order in the tilt parameter. Due to the $1/R$ dependence, this second-order tilt-dependent term would still dominate over the tilt-independent term in the limit of large R . As a consequence, the long range RKKY coupling in tilted WSMs would be determined primarily by the tilt-induced term.

In both Fig. 1(a) and 2(a), for $|\mathbf{w}| = 0.05$ the tilt induced $1/R$ term overcomes the conventional tilt-independent term (which is proportional to $1/R^3$) at around $k_F R = 40$. If a physical WSM system has Fermi energy ϵ_F such that $k_F = 1\text{\AA}^{-1}$ (i.e., $\epsilon_F = \hbar^2 k_F^2 / 2m_e = 3.43\text{ eV}$), then $k_F R = 40$ corresponds to $R = 4\text{ nm}$. This is a feasible distance to observe the RKKY coupling in practical devices and at this distance one can expect the effect of dispersion tilt in the RKKY coupling to become dominant. In addition, the direction of the dispersion tilt vector also plays an important role in the RKKY effect in tilted WSMs unlike the isotropic RKKY effect in non-tilted WSMs. For both TRS breaking and IR breaking WSMs, the sign of the RKKY magnetic ordering can change signs, i.e., from ferromagnetic to anti-ferromagnetic ordering by varying the azimuthal angle of the displacement vector \mathbf{R} between impurities with respect to the tilt vector, as shown in Fig. 1(c) and Fig. 1(c). In practical terms, this anisotropy may be utilized in modulating the sign of the RKKY exchange in layered materials, for example, where the direction of impurity displacement can be controlled. In bulk materials where the impurities are distributed isotropically, the net magnetic ordering is obtained by summing over all the displacement directions. Thus, one needs to consider the directional dependence to correctly evaluate the net sign of the RKKY coupling. This anisotropic dependence of the RKKY coupling with the tilt and separation direction has not been explored before and can shed light on the magnetic interaction between impurities and layered structures with WSMs.

V. SUMMARY

Using both the analytical method and numerical treatment we study the effect of tilt in RKKY coupling between magnetic impurities in Weyl semi-metal for both the TRS breaking and IR-breaking system. In both cases, the RKKY range function varies to the second order in the tilt parameter (at the small tilt limit). Additionally, the tilt-dependent part of the RKKY range function varies as $1/R$ with the impurity separation distance (in the limit of large R), compared to the $1/R^3$ dependence of the conventional RKKY range function in non-tilted WSMs. This means that the tilt-dependent RKKY term would dominate over the conventional tilt-independent term beyond a cross-over value of R , typically of the order of a few nano-meters which is within the practical range of RKKY coupling in experiments. Finally, the tilt-dependent term in the range function exhibits a strong anisotropy as the direction of the displacement vector \mathbf{R} is varied with respect to the tilt direction. More importantly, the sign of the coupling can change from ferromagnetic to antiferromagnetic coupling based on the displacement direction. Our analytical results were verified with numerical calculations. This work is supported by the Ministry of Education (MOE) Tier-II grant MOE2018-T2-2-117 (NUS Grant Nos. R-263-000-E45-112/R-398-000-092-112) and MOE Tier-I FRC grant (NUS Grant No. R-263-000-D66-114).

-
- [1] Shuichi Murakami. Phase transition between the quantum spin hall and insulator phases in 3d: emergence of a topological gapless phase. *New Journal of Physics*, 9(9):356, 2007.
 - [2] Xiangang Wan, Ari M. Turner, Ashvin Vishwanath, and Sergey Y. Savrasov. Topological semimetal and fermi-arc surface states in the electronic structure of pyrochlore iridates. *Phys. Rev. B*, 83:205101, May 2011.
 - [3] D. J. Thouless, M. Kohmoto, M. P. Nightingale, and M. den Nijs. Quantized hall conductance in a two-dimensional periodic potential. *Phys. Rev. Lett.*, 49:405–408, Aug 1982.
 - [4] Frank Arnold, Chandra Shekhar, Shu-Chun Wu, Yan Sun, Ricardo Donizeth dos Reis, Nitesh Kumar, Marcel Naumann, Mukkattu O. Ajeesh, Marcus Schmidt, Adolfo G. Grushin, Jens H. Bardarson, Michael Baenitz, Dmitry Sokolov, Horst Borrmann, Michael Nicklas, Claudia Felser, Elena Hassinger, and Binghai Yan. Negative magnetoresistance without well-defined chirality in the weyl semimetal tap. *Nature Communications*, 7:11615 EP –, May 2016. Article.
 - [5] Cai-Zhen Li, Li-Xian Wang, Haiwen Liu, Jian Wang, Zhi-Min Liao, and Da-Peng Yu. Giant negative magnetoresistance induced by the chiral anomaly in individual cd3as2 nanowires. *Nature Communications*, 6:10137 EP –, Dec 2015. Article.
 - [6] Qiang Li, Dmitri E. Kharzeev, Cheng Zhang, Yuan Huang, I. Pletikoscic, A. ?. V. Fedorov, R. ?. D. Zhong, J. ?. A. Schneeloch, G. ?. D. Gu, and T. Valla. Chiral magnetic effect in zrte5. *Nature Physics*, 12:550 EP –, Feb 2016.
 - [7] Xiaochun Huang, Lingxiao Zhao, Yujia Long, Peipei Wang, Dong Chen, Zhanhai Yang, Hui Liang, Mianqi Xue, Hongming Weng, Zhong Fang, Xi Dai, and Genfu Chen. Observation of the chiral-anomaly-induced negative magnetoresistance in 3d weyl semimetal taas. *Phys. Rev. X*, 5:031023, Aug 2015.
 - [8] Jun Xiong, Satya K. Kushwaha, Tian Liang, Jason W. Krizan, Max Hirschberger, Wudi Wang, R. J. Cava, and N. P. Ong. Evidence for the chiral anomaly in the dirac semimetal na3bi. *Science*, 350(6259):413–416, 2015.

- [9] Cheng-Long Zhang, Su-Yang Xu, Ilya Belopolski, Zhujun Yuan, Ziquan Lin, Bingbing Tong, Guang Bian, Nasser Alidoust, Chi-Cheng Lee, Shin-Ming Huang, Tay-Rong Chang, Guoqing Chang, Chuang-Han Hsu, Horng-Tay Jeng, Madhab Neupane, Daniel S. Sanchez, Hao Zheng, Junfeng Wang, Hsin Lin, Chi Zhang, Hai-Zhou Lu, Shun-Qing Shen, Titus Neupert, M. Zahid Hasan, and Shuang Jia. Signatures of the adler-bell-jackiw chiral anomaly in a weyl fermion semimetal. *Nature Communications*, 7:10735 EP –, Feb 2016. Article.
- [10] Yago Ferreira, A. A. Zyuzin, and Jens H. Bardarson. Anomalous nernst and thermal hall effects in tilted weyl semimetals. *Phys. Rev. B*, 96:115202, Sep 2017.
- [11] S. P. Mukherjee and J. P. Carbotte. Absorption of circular polarized light in tilted type-i and type-ii weyl semimetals. *Phys. Rev. B*, 96:085114, Aug 2017.
- [12] Da Ma, Hua Jiang, Haiwen Liu, and X. C. Xie. Planar hall effect in tilted weyl semimetals. *Phys. Rev. B*, 99:115121, Mar 2019.
- [13] S. Nandy, Girish Sharma, A. Taraphder, and Sumanta Tewari. Chiral anomaly as the origin of the planar hall effect in weyl semimetals. *Phys. Rev. Lett.*, 119:176804, Oct 2017.
- [14] Anirban Kundu, Zhuo Bin Siu, Hyunsoo Yang, and Mansoor B A Jalil. Magnetotransport of weyl semimetals with tilted dirac cones. *New Journal of Physics*, 22(8):083081, aug 2020.
- [15] S. M. Rafi-Ul-Islam, Zhuo Bin Siu, Chi Sun, and Mansoor B. A. Jalil. Strain-controlled current switching in weyl semimetals. *Phys. Rev. Applied*, 14:034007, Sep 2020.
- [16] Can Yesilyurt, Seng Ghee Tan, Gengchiao Liang, and Mansoor B. A. Jalil. Klein tunneling in weyl semimetals under the influence of magnetic field. *Scientific Reports*, 6(1):38862, Dec 2016.
- [17] Ben-Chuan Lin, Shuo Wang, An-Qi Wang, Ying Li, Rong-Rong Li, Ke Xia, Dapeng Yu, and Zhi-Min Liao. Electric control of fermi arc spin transport in individual topological semimetal nanowires. *Phys. Rev. Lett.*, 124:116802, Mar 2020.
- [18] Vardan Kaladzhyan and Jens H. Bardarson. Quantized fermi arc mediated transport in weyl semimetal nanowires. *Phys. Rev. B*, 100:085424, Aug 2019.
- [19] Andrew K. Mitchell and Lars Fritz. Kondo effect in three-dimensional dirac and weyl systems. *Phys. Rev. B*, 92:121109, Sep 2015.
- [20] Alessandro Principi, Giovanni Vignale, and E. Rossi. Kondo effect and non-fermi-liquid behavior in dirac and weyl semimetals. *Phys. Rev. B*, 92:041107, Jul 2015.
- [21] Pavan Hosur. Friedel oscillations due to fermi arcs in weyl semimetals. *Phys. Rev. B*, 86:195102, Nov 2012.
- [22] Shengyuan A. Yang, Hui Pan, and Fan Zhang. Dirac and weyl superconductors in three dimensions. *Phys. Rev. Lett.*, 113:046401, Jul 2014.
- [23] Yanpeng Qi, Pavel G. Naumov, Mazhar N. Ali, Catherine R. Rajamathi, Walter Schnelle, Oleg Barkalov, Michael Hanfland, Shu-Chun Wu, Chandra Shekhar, Yan Sun, Vicky Süß, Marcus Schmidt, Ulrich Schwarz, Eckhard Pippel, Peter Werner, Reinald Hillebrand, Tobias Förster, Erik Kampert, Stuart Parkin, R. J. Cava, Claudia Felser, Binghai Yan, and Sergey A. Medvedev. Superconductivity in weyl semimetal candidate mote2. *Nature Communications*, 7(1):11038, Mar 2016.
- [24] Maja D. Bachmann, Nityan Nair, Felix Flicker, Roni Ilan, Tobias Meng, Nirmal J. Ghimire, Eric D. Bauer, Filip Ronning, James G. Analytis, and Philip J. W. Moll. Inducing superconductivity in weyl semimetal microstructures by selective ion sputtering. *Science Advances*, 3(5), 2017.
- [25] Bo Lu, Keiji Yada, Masatoshi Sato, and Yukio Tanaka. Crossed surface flat bands of weyl semimetal superconductors. *Phys. Rev. Lett.*, 114:096804, Mar 2015.
- [26] A. A. Burkov. Anomalous hall effect in weyl metals. *Phys. Rev. Lett.*, 113:187202, Oct 2014.
- [27] Qi Wang, Yuanfeng Xu, Rui Lou, Zhonghao Liu, Man Li, Yaobo Huang, Dawei Shen, Hongming Weng, Shancai Wang, and Hechang Lei. Large intrinsic anomalous hall effect in half-metallic ferromagnet $\text{Co}_3\text{Sn}_2\text{S}_2$ with magnetic weyl fermions. *Nature Communications*, 9(1):3681, Sep 2018.
- [28] B. Q. Lv, H. M. Weng, B. B. Fu, X. P. Wang, H. Miao, J. Ma, P. Richard, X. C. Huang, L. X. Zhao, G. F. Chen, Z. Fang, X. Dai, T. Qian, and H. Ding. Experimental discovery of weyl semimetal taas. *Phys. Rev. X*, 5:031013, Jul 2015.
- [29] B. Q. Lv, N. Xu, H. M. Weng, J. Z. Ma, P. Richard, X. C. Huang, L. X. Zhao, G. F. Chen, C. E. Matt, F. Bisti, V. N. Strocov, J. Mesot, Z. Fang, X. Dai, T. Qian, M. Shi, and H. Ding. Observation of weyl nodes in taas. *Nature Physics*, 11:724 EP –, Aug 2015.
- [30] Su-Yang Xu, Ilya Belopolski, Nasser Alidoust, Madhab Neupane, Guang Bian, Chenglong Zhang, Raman Sankar, Guoqing Chang, Zhujun Yuan, Chi-Cheng Lee, Shin-Ming Huang, Hao Zheng, Jie Ma, Daniel S. Sanchez, BaoKai Wang, Arun Bansil, Fangcheng Chou, Pavel P. Shibayev, Hsin Lin, Shuang Jia, and M. Zahid Hasan. Discovery of a weyl fermion semimetal and topological fermi arcs. *Science*, 349(6248):613–617, 2015.
- [31] N. Xu, H. M. Weng, B. Q. Lv, C. E. Matt, J. Park, F. Bisti, V. N. Strocov, D. Gawryluk, E. Pomjakushina, K. Conder, N. C. Plumb, M. Radovic, G. Autès, O. V. Yazyev, Z. Fang, X. Dai, T. Qian, J. Mesot, H. Ding, and M. Shi. Observation of weyl nodes and fermi arcs in tantalum phosphide. *Nature Communications*, 7:11006 EP –, Mar 2016. Article.
- [32] Shin-Ming Huang, Su-Yang Xu, Ilya Belopolski, Chi-Cheng Lee, Guoqing Chang, BaoKai Wang, Nasser Alidoust, Guang Bian, Madhab Neupane, Chenglong Zhang, Shuang Jia, Arun Bansil, Hsin Lin, and M. Zahid Hasan. A weyl fermion semimetal with surface fermi arcs in the transition metal monpnictide taas class. *Nature Communications*, 6(1):7373, Jun 2015.
- [33] Hao-Ran Chang, Jianhui Zhou, Shi-Xiong Wang, Wen-Yu Shan, and Di Xiao. Rkky interaction of magnetic impurities in dirac and weyl semimetals. *Phys. Rev. B*, 92:241103, Dec 2015.
- [34] Hou-Jian Duan, Shi-Han Zheng, Rui-Qiang Wang, Ming-Xun Deng, and Mou Yang. Signature of indirect magnetic interaction in the crossover from type-i to type-ii weyl semimetals. *Phys. Rev. B*, 99:165111, Apr 2019.

- [35] Avinash Singh, Animesh Datta, Subrat K. Das, and Vijay A. Singh. Ferromagnetism in a dilute magnetic semiconductor: Generalized rkk interaction and spin-wave excitations. *Phys. Rev. B*, 68:235208, Dec 2003.
- [36] C. H. Ziener, S. Glutsch, and F. Bechstedt. Rkky interaction in semiconductors: Effects of magnetic field and screening. *Phys. Rev. B*, 70:075205, Aug 2004.
- [37] Sonu Verma, Arijit Kundu, and Tarun Kanti Ghosh. Rkky interaction in mn-doped 4×4 luttinger systems. *Journal of Applied Physics*, 125(23):233903, 2019.
- [38] Cong Son Ho, Seng Ghee Tan, Zhuo Bin Siu, and Mansoor B A Jalil. Zitterbewegung-mediated RKKY coupling in topological insulator thin films. *New Journal of Physics*, 22(7):073019, jul 2020.
- [39] Cong Son Ho and Mansoor B. A. Jalil. Effect of surface hybridization on rkk coupling in ferromagnet/topological insulator/ferromagnet trilayer system. *AIP Advances*, 7(5):055926, 2017.
- [40] A. A. Zyuzin and R. P. Tiwari. Intrinsic anomalous hall effect in type-ii weyl semimetals. *JETP Letters*, 103(11):717–722, Jun 2016.
- [41] Zhi-Ming Yu, Yugui Yao, and Shengyuan A. Yang. Predicted unusual magnetoresponse in type-ii weyl semimetals. *Phys. Rev. Lett.*, 117:077202, Aug 2016.
- [42] M. Udagawa and E. J. Bergholtz. Field-selective anomaly and chiral mode reversal in type-ii weyl materials. *Phys. Rev. Lett.*, 117:086401, Aug 2016.
- [43] Mir Vahid Hosseini and Mehdi Askari. Ruderman-kittel-kasuya-yosida interaction in weyl semimetals. *Phys. Rev. B*, 92:224435, Dec 2015.
- [44] M. O. Goerbig, J.-N. Fuchs, G. Montambaux, and F. Piéchon. Tilted anisotropic dirac cones in quinoid-type graphene and α -(BEDT-TTF)₂I₃. *Phys. Rev. B*, 78:045415, Jul 2008.
- [45] Hiroshi Imamura, Patrick Bruno, and Yasuhiro Utsumi. Twisted exchange interaction between localized spins embedded in a one- or two-dimensional electron gas with rashba spin-orbit coupling. *Phys. Rev. B*, 69:121303, Mar 2004.

Supplemental material for "Ruderman-Kittel-Kasuya-Yosida (RKKY) interaction in
Weyl semimetals with tilted energy dispersion"

Anirban Kundu^{1,2} and M. B. A. Jalil¹

¹*Department of Electrical and Computer Engineering,
National University of Singapore, 4 Engineering Drive 3, Singapore 117576*

²*Physics Department, Ariel University, Ariel 40700, Israel*

I. METHOD

RKKY term: The magnetic interaction between conduction electrons and the impurity can perturbation term can be written as,

$$H' = J \sum_i \mathbf{S}_i \cdot \sigma \delta(\mathbf{r} - \mathbf{R}_i) = J [\sigma \cdot \mathbf{S}_1 \delta(\mathbf{r} - \mathbf{R}_1) + \sigma \cdot \mathbf{S}_2 \delta(\mathbf{r} - \mathbf{R}_2)] \quad (S1)$$

$$\begin{aligned} \langle \mathbf{k}'\eta | H' | \mathbf{k}\eta' \rangle &= (J/V) \int d\mathbf{r} e^{i(\mathbf{k}' - \mathbf{Q}) \cdot \mathbf{r}} [\sigma \cdot \mathbf{S}_1 \delta(\mathbf{r} - \mathbf{R}_1) + \sigma \cdot \mathbf{S}_2 \delta(\mathbf{r} - \mathbf{R}_2)] e^{-i(\mathbf{k} + \mathbf{Q}) \cdot \mathbf{r}} \\ &= (J/V) \left[\sigma \cdot \mathbf{S}_1 e^{i(\mathbf{k}' - \mathbf{k} - 2\mathbf{Q}) \cdot \mathbf{R}_1} + \sigma \cdot \mathbf{S}_2 e^{i(\mathbf{k}' - \mathbf{k} - 2\mathbf{Q}) \cdot \mathbf{R}_2} \right], \end{aligned} \quad (S2)$$

$$|\langle \mathbf{k}\eta | H' | \mathbf{k}'\eta' \rangle|^2 (J/V)^2 = (\mathbf{S}_1)^2 + (\mathbf{S}_2)^2 + 2(\mathbf{S}_1 \cdot \mathbf{S}_2) \cos[(\mathbf{k}' - \mathbf{k} - 2\mathbf{Q}) \cdot \mathbf{R}], \quad (S3)$$

where $\mathbf{q} = \mathbf{k} - \mathbf{k}'$ and $\mathbf{R} = \mathbf{R}_1 - \mathbf{R}_2$. The energy difference between two bands:

$$\epsilon_{\mathbf{k}', \eta', c} - \epsilon_{\mathbf{k}, \eta, c} = \hbar v_F (\eta' c' |\mathbf{k}' - \eta' \mathbf{Q}| - \eta c |\mathbf{k} - \eta \mathbf{Q}|) + \hbar v_F \mathbf{w}_{\eta'} \cdot (\mathbf{k}' - \eta' \mathbf{Q}) - \hbar v_F \mathbf{w}_\eta \cdot (\mathbf{k} - \eta \mathbf{Q}) + (\eta' - \eta) \hbar v_F Q_0. \quad (S4)$$

Now considering that the Fermi energy $\epsilon_F > 0$, only the $\eta = 1, c = 1$ and $\eta = -1, c = -1$ are relevant. Using the above condition we obtain,

$$\epsilon_{\mathbf{k}', \eta'} - \epsilon_{\mathbf{k}, \eta} = \hbar v_F (|\mathbf{k}' - \eta' \mathbf{Q}| - |\mathbf{k} - \eta \mathbf{Q}|) + \hbar v_F \mathbf{w}_{\eta'} \cdot (\mathbf{k}' - \eta' \mathbf{Q}) - \hbar v_F \mathbf{w}_\eta \cdot (\mathbf{k} - \eta \mathbf{Q}) + (\eta' - \eta) \hbar v_F Q_0. \quad (S5)$$

The second order correction is $\epsilon^{(2)} = 2(\mathbf{S}_1 \cdot \mathbf{S}_2) F(R)$, with,

$$F(R) = \sum_\eta F_{\text{intra}}(\eta, R) + \sum_{\eta' \neq \eta} e^{i(\eta 2\mathbf{Q} \cdot \mathbf{R})} F_{\text{inter}}(\eta, -\eta, R), \quad (S6)$$

where, for intra-valley: $(\epsilon_{\mathbf{k}', \eta} - \epsilon_{\mathbf{k}, \eta}) = \hbar v_F (|\mathbf{k}' - \eta \mathbf{Q}| - |\mathbf{k} - \eta \mathbf{Q}|) + \hbar \mathbf{w}_\eta \cdot (\mathbf{k}' - \eta \mathbf{Q}) - \hbar \mathbf{w}_\eta \cdot (\mathbf{k} - \eta \mathbf{Q})$ and we obtain

$$\begin{aligned} F_{\text{intra}}(\eta, R) &= \text{Re} \left(\frac{1}{\hbar v_F} \right) \int_{|\mathbf{k} - \eta \mathbf{Q}|=0}^{k_{F\eta}} d\mathbf{k} \int_{|\mathbf{k}' - \eta \mathbf{Q}|=k_{F\eta}}^{\infty} d\mathbf{k}' \frac{e^{i(\mathbf{k}' - \mathbf{k}) \cdot \mathbf{R}}}{\epsilon_{\mathbf{k}'\eta} - \epsilon_{\mathbf{k}\eta}} \\ &= \text{Re} \left(\frac{1}{\hbar v_F} \right) \int_{k=0}^{k_{F\eta}} d\mathbf{k} \int_{k'=k_{F\eta}}^{\infty} d\mathbf{k}' \frac{e^{i(\mathbf{k}' - \mathbf{k}) \cdot \mathbf{R}}}{(k' - k) + \frac{\mathbf{w}_\eta}{v_F} \cdot (\mathbf{k}' - \mathbf{k})}. \end{aligned} \quad (S7)$$

In the last line above we substituted $(\mathbf{k}' - \eta \mathbf{Q}) \rightarrow \mathbf{k}'$ and $(\mathbf{k} - \eta \mathbf{Q}) \rightarrow \mathbf{k}$ without loss of any generality. For inter-valley ($\eta' \neq \eta$) the energy difference becomes $(\epsilon_{\mathbf{k}', \eta'} - \epsilon_{\mathbf{k}, \eta}) = \hbar v_F (|\mathbf{k}' - \eta' \mathbf{Q}| - |\mathbf{k} - \eta \mathbf{Q}|) + \hbar \mathbf{w}_{\eta'} \cdot (\mathbf{k}' - \eta' \mathbf{Q}) - \hbar \mathbf{w}_\eta \cdot (\mathbf{k} - \eta \mathbf{Q}) + (\eta' - \eta) \hbar v_F Q_0$

$$F_{\text{inter}}(\eta, \eta', R) = \text{Re} \int_0^{k_{F\eta}} d\mathbf{k} \int_{k_{F\eta'}}^{\infty} d\mathbf{k}' \frac{e^{i(\mathbf{k}' - \mathbf{k}) \cdot \mathbf{R}}}{\epsilon_{\mathbf{k}'\eta'} - \epsilon_{\mathbf{k}\eta}} \quad (S8)$$

$$\begin{aligned} &= \text{Re} \int_{|\mathbf{k} - \eta \mathbf{Q}|=0}^{k_{F\eta}} d\mathbf{k} \int_{|\mathbf{k}' - \eta' \mathbf{Q}|=k_{F\eta'}}^{\infty} d\mathbf{k}' \\ &\times \left[\frac{e^{i(\mathbf{k}' - \mathbf{k}) \cdot \mathbf{R}}}{\hbar v_F (|\mathbf{k}' - \eta' \mathbf{Q}| - |\mathbf{k} - \eta \mathbf{Q}|) + \hbar \mathbf{w}_{\eta'} \cdot (\mathbf{k}' - \eta' \mathbf{Q}) - \hbar \mathbf{w}_\eta \cdot (\mathbf{k} - \eta \mathbf{Q}) + (\eta' - \eta) \hbar v_F Q_0} \right] \end{aligned} \quad (S9)$$

$$= \text{Re} \int_{k=0}^{k_{F\eta}} d\mathbf{k} \int_{k'=k_{F\eta'}}^{\infty} d\mathbf{k}' \frac{e^{i(\mathbf{k}' - \mathbf{k}) \cdot \mathbf{R}}}{\hbar v_F (k' - k) + \hbar (\mathbf{w}_{\eta'} \cdot \mathbf{k}' - \mathbf{w}_\eta \cdot \mathbf{k}) + (\eta' - \eta) \hbar v_F Q_0}. \quad (S10)$$

Finally we can write using $\eta' = -\eta$,

$$F_{\text{inter}}(\eta, -\eta, R) = \text{Re} \int_{k=0}^{k_{F\eta}} d\mathbf{k} \int_{k'=k_{F-\eta}}^{\infty} d\mathbf{k}' \frac{e^{i(\mathbf{k}'-\mathbf{k})\cdot\mathbf{R}}}{\hbar v_F(k'-k) + \hbar(\mathbf{w}_{\mp}\cdot\mathbf{k}' - \hbar v_F \mathbf{w}_{\pm}\cdot\mathbf{k}) - \eta 2\hbar v_F q_0}. \quad (\text{S11})$$

II. SMALL TILT LIMIT

As stated before,

$$F(R) = \sum_{\eta} F_{\text{intra}}(\eta, R) + \sum_{\eta' \neq \eta} e^{i(\eta 2\mathbf{Q}\cdot\mathbf{R})} F_{\text{inter}}(\eta, -\eta, R), \quad (\text{S12})$$

Expanding to the second order in tilt:

$$F_{\text{intra}}(\eta, R) = \text{Re} \int_{k=0}^{k_{F\eta}} d\mathbf{k} \int_{k'=k_{F\eta}}^{\infty} d\mathbf{k}' \frac{e^{i(\mathbf{k}'-\mathbf{k})\cdot\mathbf{R}}}{\hbar v_F(k'-k)} + \text{Re} \int_{k=0}^{k_{F\eta}} d\mathbf{k} \int_{k'=k_{F\eta}}^{\infty} d\mathbf{k}' \frac{(\mathbf{w}_{\eta}\cdot\mathbf{k}' - \mathbf{w}_{-\eta}\cdot\mathbf{k})^2 e^{i(\mathbf{k}'-\mathbf{k})\cdot\mathbf{R}}}{\hbar v_F(k'-k)^3} \quad (\text{S13})$$

$$= \sum_{m=0}^2 \left(\frac{\mathbf{w}_{\pm}}{v_F} \cdot \frac{\partial}{\partial \mathbf{R}} \right)^m \chi^{(m)}(\mathbf{R}), \quad (\text{S14})$$

where,

$$\chi^{(m)}(\mathbf{R}) = \left(\frac{1}{\hbar v_F} \right) \text{Re} (-i)^m \int_0^{k_{F\eta}} d\mathbf{k} \int_{k_{F\eta}}^{\infty} d\mathbf{k}' \frac{e^{i(\mathbf{k}'-\mathbf{k})\cdot\mathbf{R}}}{(k'-k)^{m+1}}. \quad (\text{S15})$$

And the inter-valley range function becomes,

$$F_{\text{inter}}^{\eta, -\eta}(\mathbf{R}) = \sum_{m=0}^2 \zeta^{(m, \eta, -\eta)}(\mathbf{R}), \quad (\text{S16})$$

where,

$$\zeta^{(m, \eta, -\eta)}(\mathbf{R}) = \text{Re} \int_{k=0}^{k_{F\eta}} d\mathbf{k} \int_{k'=k_{F, -\eta}}^{\infty} d\mathbf{k}' \frac{\hbar^m (\mathbf{w}_{\eta}\cdot\mathbf{k}' - \mathbf{w}_{-\eta}\cdot\mathbf{k})^m e^{i(\mathbf{k}'-\mathbf{k})\cdot\mathbf{R}}}{(\hbar v_F(k'-k) \mp 2\epsilon_0)^{m+1}}. \quad (\text{S17})$$

Clearly for chiral tilt i.e., $\mathbf{w}_{\pm} = \pm\mathbf{w}$ the second term vanishes after summing over the contribution for a pair of nodes. Also the imaginary part of the integration $\text{Im}[\dots]$ is zero, meaning that for $\mathbf{w}_{\pm} = \mathbf{w}$ the linear in tilt term vanishes. Finally we obtain in general for intra-valley, putting $q_0 = 0$ in the above case leads to the coupling for TRS symmetry breaking case, however $q_0 \neq 0$ implies IR symmetry breaking case. Results for parallel tilt ($\mathbf{w}_{\eta} = \mathbf{w}$),

A. TRS broken ($\epsilon_0 = 0$ and $\mathbf{Q} \neq 0$)

The Hamiltonian in that scenario is, $H_0 = \eta v_F \tau \cdot (\mathbf{k} - \eta \mathbf{Q}) + \eta \mathbf{w} \cdot (\mathbf{k} - \eta \mathbf{Q}) \tau_0$ and $k_{F\eta} = k_F = \epsilon_F / \hbar v_F$ we get

$$F_{\text{intra}}(\eta, R) = \text{Re} \int_{k=0}^{k_{F\eta}} d\mathbf{k} \int_{k'=k_{F\eta}}^{\infty} d\mathbf{k}' \frac{e^{i(\mathbf{k}'-\mathbf{k})\cdot\mathbf{R}}}{\hbar v_F(k'-k)} + \hbar(\mathbf{w} \cdot \nabla_{\mathbf{R}})^2 \text{Re} \int_{k=0}^{k_{F\eta}} d\mathbf{k} \int_{k'=k_{F\eta}}^{\infty} d\mathbf{k}' \frac{e^{i(\mathbf{k}'-\mathbf{k})\cdot\mathbf{R}}}{[\hbar v_F(k'-k)]^3} \quad (\text{S18})$$

$$= \sum_{m=0}^2 \left(\frac{\mathbf{w}}{v_F} \cdot \frac{\partial}{\partial \mathbf{R}} \right)^m \chi^{(m, \eta)}(R), \quad (\text{S19})$$

where,

$$\chi^{(m,\eta)}(R) = \left(\frac{1}{\hbar v_F}\right) \text{Re}(-i)^m \int_0^{k_F} d\mathbf{k} \int_{k_F}^{\infty} d\mathbf{k}' \frac{e^{i(\mathbf{k}'-\mathbf{k})\cdot\mathbf{R}}}{(k'-k)^{m+1}}, \quad (\text{S20})$$

$$\zeta^{(m)}(\eta, -\eta, R) = \text{Re} \int_{k=0}^{k_F\eta} d\mathbf{k} \int_{k'=k_F-\eta}^{\infty} d\mathbf{k}' \frac{\hbar^m (\mathbf{w}\cdot\mathbf{k}' - \mathbf{w}\cdot\mathbf{k})^m e^{i(\mathbf{k}'-\mathbf{k})\cdot\mathbf{R}}}{[\hbar v_F (k'-k)]^{m+1}} \quad (\text{S21})$$

$$= \left(\frac{1}{\hbar v_F}\right) \left(\frac{\mathbf{w}}{v_F} \cdot \frac{\partial}{\partial \mathbf{R}}\right)^m \text{Re}(-i)^m \int_{k=0}^{k_F} d\mathbf{k} \int_{k'=k_F}^{\infty} d\mathbf{k}' \frac{e^{i(\mathbf{k}'-\mathbf{k})\cdot\mathbf{R}}}{(k'-k)^{m+1}} \quad (\text{S22})$$

$$= \left(\frac{\mathbf{w}}{v_F} \cdot \frac{\partial}{\partial \mathbf{R}}\right)^m \chi^{(m,\eta)}(R) \quad (\text{S23})$$

The inter contribution is,

$$F_{\text{inter}}^{\eta,-\eta}(\mathbf{R}) = \left(\frac{\mathbf{w}}{v_F} \cdot \frac{\partial}{\partial \mathbf{R}}\right)^m \chi^{(m,\eta)}(R) \quad (\text{S24})$$

So, the total range function is,

$$F(\mathbf{R}) = \sum_{\eta} F_{\text{intra}}^{\eta}(\mathbf{R}) + \sum_{\eta} e^{i(\eta 2\mathbf{Q}\cdot\mathbf{R})} F_{\text{inter}}^{\eta,-\eta}(\mathbf{R}). \quad (\text{S25})$$

$$= 2(1 + \cos(2\mathbf{Q}\cdot\mathbf{R})) \left(\chi^{(0,\eta)}(R) - \left(\frac{\mathbf{w}}{v_F} \cdot \frac{\partial}{\partial \mathbf{R}}\right)^2 \chi^{(2,\eta)}(R) \right) \quad (\text{S26})$$

B. IR-broken ($\mathbf{Q} = 0$ and $\epsilon \neq 0$)

The Hamiltonian is: $H_0 = \eta v_F \tau \cdot \mathbf{k} + \mathbf{w}_\eta \cdot \mathbf{k} \tau_0 + \eta Q_0 \tau_0$. The total range function,

$$F^{IR}(\mathbf{R}) = \left\{ \sum_{\eta} \chi_{IR}^{(0,\eta)}(R) - \sum_{\eta} \left(\frac{\mathbf{w}}{v_F} \cdot \frac{\partial}{\partial \mathbf{R}}\right)^2 \chi_{IR}^{(2,\eta)}(R) \right\} + \left\{ \sum_{\eta} \left[\zeta_{IR}^{(0)}(\eta, -\eta, R) - \left(\frac{\mathbf{w}}{v_F} \cdot \frac{\partial}{\partial \mathbf{R}}\right)^2 \zeta_{IR}^{(2)}(\eta, -\eta, R) \right] \right\}, \quad (\text{S27})$$

and we introduce,

$$\chi^{(n,\pm)}(R) = \left(\frac{1}{\hbar v_F}\right) \text{Re} \left[(-i)^n \int_0^{k_{F\pm}} d\mathbf{k} \int_{k_{F\pm}}^{\infty} d\mathbf{k}' \frac{e^{i(\mathbf{k}'-\mathbf{k})\cdot\mathbf{R}}}{(k'-k)^{n+1}} \right], \quad (\text{S28})$$

and

$$\zeta_{IR}^{(n)}(\eta, -\eta, R) = \text{Re} \int_{k=0}^{k_F \eta} d\mathbf{k} \int_{k'=k_{F\eta'}}^{\infty} dk' \frac{e^{i(\mathbf{k}'-\mathbf{k})\cdot\mathbf{R}}}{(k'-k) \mp 2q_0^{n+1}} \quad (\text{S29})$$

$$\text{using, } \int d\mathbf{k} = \int dk k^2 \int d\theta \sin\theta \int d\phi = \int dk k^2 \int_{-1}^1 dx \int d\phi =$$

$$= \left(\frac{4\pi}{R}\right)^2 \int_0^{k_{F\eta}} dk (k \sin kR) \int_{k_{F\eta}}^{\infty} dk' \frac{k' \sin k'R}{(k'-k \pm 2q_0)}$$

$$\text{Rescale } k \rightarrow k - \eta q_0 \text{ such that } \int_0^{k_{F\pm}} dk \rightarrow \int_0^{k_F} dk \text{ cause } k_F = k_{F\pm} + \eta q_0$$

$$= \left(\frac{4\pi}{R}\right)^2 \int_0^{k_F} dk (k - \eta q_0) \sin[(k - \eta q_0)R] \int_{k_F}^{\infty} dk' \frac{(k' \pm q_0) \sin[(k' + \eta q_0)R]}{(k' - k)^3} \quad (\text{S30})$$

$$= \left(\frac{4\pi}{R}\right)^2 \int_0^{k_F} dk (k - \eta q_0) \sin[(k - \eta q_0)R] \int_0^{\infty} dk' \frac{(k' \pm q_0) \sin[(k' + \eta q_0)R]}{(k' - k)^3}. \quad (\text{S31})$$

After contour integration,

$$\begin{aligned} \sum_{\eta} \chi_{IR}^{(0,\eta)}(R) &= \frac{2\pi^2 \left((1 - 2R^2(k_F - q_0)^2) \cos(2R(k_F - q_0)) + (1 - 2R^2(k_F + q_0)^2) \cos(2R(k_F + q_0)) \right)}{R^5} \\ &+ \frac{2\pi^2 \left(+2R(k_F - q_0) \sin(2R(k_F - q_0)) + 2R(k_F + q_0) \sin(2R(k_F + q_0)) - 2 \right)}{R^5}, \end{aligned} \quad (\text{S32})$$

$$\sum_{\eta} \zeta^{(0,\eta,-\eta)}(R) = \frac{\pi \left((1 - 2R^2(k_F - q_0)(k_F + q_0)) \cos(2k_F R) + 2k_F R \sin(2k_F R) - 2q_0^2 R^2 - 1 \right)}{2R^3}, \quad (\text{S33})$$

$$\begin{aligned} &\sum_{\eta} \chi_{IR}^{(0,\eta)}(R) + \sum_{\eta} \zeta^{(0,\eta,-\eta)}(R) \\ &= \frac{2\pi^2 \left(2(1 - 2R^2(k_F - q_0)(k_F + q_0)) \cos(2k_F R) + (1 - 2R^2(k_F - q_0)^2) \cos(2R(k_F - q_0)) \right)}{R^5} \\ &+ \frac{2\pi^2 \left((1 - 2R^2(k_F + q_0)^2) \cos(2R(k_F + q_0)) + 2R(k_F - q_0) \sin(2R(k_F - q_0)) \right)}{R^5} \\ &+ \frac{2\pi^2 \left(2R(k_F + q_0) \sin(2R(k_F + q_0)) + 4k_F R \sin(2k_F R) - 4q_0^2 R^2 - 4 \right)}{R^5}. \end{aligned} \quad (\text{S34})$$

Contribution from the tilt,

$$\chi_{IR}^{(2,\eta)}(R) = \frac{4\pi^3 \left(-4R^2(q_F - \eta q_0)^2 + (2R^2(q_F - \eta q_0)^2 + 1) \cos(2R(q_F - \eta q_0)) + 2R(q_F - \eta q_0) \sin(2R(q_F - \eta q_0)) - 1 \right)}{R^3}, \quad (\text{S35})$$

$$\begin{aligned} \zeta_{IR}^{(2)}(\eta, -\eta, R) &= \frac{4\pi^3 \left(2R(3\eta q_0 - 2R^2(k_F - 4\eta q_0)(k_F - \eta q_0)^2) \sin(2\eta q_0 R) - 3(4R^2(k_F - \eta q_0)^2 + 1) \cos(2\eta q_0 R) \right)}{3R^3} \\ &+ \frac{4\pi^3 \left(3(2R^2(k_F - \eta q_0)(k_F - 3\eta q_0) + 1) \cos(2R(k_F - 2\eta q_0)) + 6k_F R \sin(2R(k_F - 2\eta q_0)) \right)}{3R^3}. \end{aligned} \quad (\text{S36})$$

For $\mathbf{w} \parallel \hat{z}$

$$\begin{aligned}
& \left(\frac{|\mathbf{w}|}{v_F} \cdot \frac{\partial}{\partial R_z} \right)^2 \chi_{IR}^{(2,\eta)}(\mathbf{R}) \\
&= - \frac{2\pi^3 (R^2 (-4 (R^2 - 3R_z^2) (k_F - \eta q_0)^2 - 3) + 15R_z^2)}{R^7} \\
& - \frac{2\pi^3 (+2R(k_F - \eta q_0) \sin(2R(k_F - \eta q_0)) (R^2 (2(R - R_z)(R + R_z)(k_F - \eta q_0)^2 + 3) - 15R_z^2))}{R^7} \\
& - \frac{2\pi^3 (\cos(2R(k_F - \eta q_0)) (R^2 (2(k_F - \eta q_0)^2 (R^2(2k_F R_z - 2\eta q_0 R_z - 1)(2k_F R_z - 2\eta q_0 R_z + 1) + 9R_z^2) + 3) - 15R_z^2))}{R^7}, \tag{S37}
\end{aligned}$$

and

$$\begin{aligned}
& \left(\frac{|\mathbf{w}|}{v_F} \cdot \frac{\partial}{\partial R_z} \right)^2 \zeta_{IR}^{(2)}(\eta, -\eta, \mathbf{R}) \\
&= \frac{2\pi^3 (-3 \cos(2k_F R) (R^2 (2z^2 (9k_F^2 - 20\eta k_F q_0 + 3\eta^2 q_0^2) + 3) + R^4 (8k_F^4 z^2 - 2\eta^2 q_0^2 (4k_F^2 z^2 + 1) - 2k_F^2 + 8\eta k_F q_0) - 15z^2))}{3R^7} \\
& + \frac{2\pi^3 (3R^2 (3 - 2\eta^2 q_0^2 (R^2 - 3z^2)) - 45z^2)}{3R^7} \\
& + \frac{2\pi^3 (4k_F R^2 \cos(2\eta q_0 R) (2\eta q_0 (R^2 (k_F^2 (R - z)(R + z) - 3) + 9z^2) + 12\eta^2 k_F q_0^2 R^2 z^2 + 3k_F (R^2 - 3z^2) - 6\eta^3 q_0^3 R^2 (R^2 + 3z^2)))}{3R^7} \\
& \frac{2\pi^3 (-8\eta k_F q_0 R^3 \sin(2\eta q_0 R) (2\eta q_0 (R^2 (k_F^2 z^2 + 3) - 9z^2) - 3k_F (R^2 - 3z^2) - 6\eta^3 q_0^3 R^2 z^2))}{3R^7} \\
& \frac{2\pi^3 (-6R \sin(2k_F R) (2k_F^3 R^2 (R - z)(R + z) - 4\eta q_0 (2z^2 (k_F^2 R^2 - 2) + R^2) - 2\eta^2 k_F q_0^2 R^2 (R^2 - 3z^2) + 3k_F (R^2 - 5z^2)))}{3R^7}. \tag{S38}
\end{aligned}$$

Finally the full expression for range function for IR broken system is as follows,

$$\begin{aligned}
F^{IR}(\mathbf{R}) &= \frac{2\pi^2 \left(2 \left(1 - 2R^2(k_F - q_0)(k_F + q_0) \right) \cos(2k_F R) + \left(1 - 2R^2(k_F - q_0)^2 \right) \cos(2R(k_F - q_0)) \right)}{R^5} \\
&+ \frac{2\pi^2 \left(\left(1 - 2R^2(k_F + q_0)^2 \right) \cos(2R(k_F + q_0)) + 2R(k_F - q_0) \sin(2R(k_F - q_0)) \right)}{R^5} \\
&+ \frac{2\pi^2 \left(2R(k_F + q_0) \sin(2R(k_F + q_0)) + 4k_F R \sin(2k_F R) - 4q_0^2 R^2 - 4 \right)}{R^5} \\
&+ \frac{|\mathbf{w}|^2}{v_F^2} [\dots] \\
\text{with} \\
[\dots] &= - \frac{2\pi^3 \left(R^2 \left(-4 \left(R^2 - 3R_z^2 \right) (k_F - \eta q_0)^2 - 3 \right) + 15R_z^2 \right)}{R^7} \\
&- \frac{2\pi^3 \left(+2R(k_F - \eta q_0) \sin(2R(k_F - \eta q_0)) \left(R^2 \left(2(R - R_z)(R + R_z)(k_F - \eta q_0)^2 + 3 \right) - 15R_z^2 \right) \right)}{R^7} \\
&- \frac{2\pi^3 \left(\cos(2R(k_F - \eta q_0)) \left(R^2 \left(2(k_F - \eta q_0)^2 \left(R^2(2k_F R_z - 2\eta q_0 R_z - 1)(2k_F R_z - 2\eta q_0 R_z + 1) + 9R_z^2 \right) + 3 \right) - 15R_z^2 \right) \right)}{R^7} \\
&+ \frac{2\pi^3 \left(-3 \cos(2k_F R) \left(R^2 \left(2z^2 \left(9k_F^2 - 20\eta k_F q_0 + 3\eta^2 q_0^2 \right) + 3 \right) + R^4 \left(8k_F^4 z^2 - 2\eta^2 q_0^2 \left(4k_F^2 z^2 + 1 \right) - 2k_F^2 + 8\eta k_F q_0 \right) - 15z^2 \right) \right)}{3R^7} \\
&+ \frac{2\pi^3 \left(3R^2 \left(3 - 2\eta^2 q_0^2 \left(R^2 - 3z^2 \right) \right) - 45z^2 \right)}{3R^7} \\
&+ \frac{2\pi^3 \left(4k_F R^2 \cos(2\eta q_0 R) \left(2\eta q_0 \left(R^2 \left(k_F^2 (R - z)(R + z) - 3 \right) + 9z^2 \right) + 12\eta^2 k_F q_0^2 R^2 z^2 + 3k_F \left(R^2 - 3z^2 \right) - 6\eta^3 q_0^3 R^2 \left(R^2 + 3z^2 \right) \right) \right)}{3R^7} \\
&+ \frac{2\pi^3 \left(-8\eta k_F q_0 R^3 \sin(2\eta q_0 R) \left(2\eta q_0 \left(R^2 \left(k_F^2 z^2 + 3 \right) - 9z^2 \right) - 3k_F \left(R^2 - 3z^2 \right) - 6\eta^3 q_0^3 R^2 z^2 \right) \right)}{3R^7} \\
&+ \frac{2\pi^3 \left(-6R \sin(2k_F R) \left(2k_F^3 R^2 (R - z)(R + z) - 4\eta q_0 \left(2z^2 \left(k_F^2 R^2 - 2 \right) + R^2 \right) - 2\eta^2 k_F q_0^2 R^2 \left(R^2 - 3z^2 \right) + 3k_F \left(R^2 - 5z^2 \right) \right) \right)}{3R^7}.
\end{aligned} \tag{S39}$$

III. OPPOSITELY TILTED ($\mathbf{W}_\eta = \pm \mathbf{W}$)

TRS broken ($Q_0 = 0$):

$$\chi^{(2,\eta)}(\mathbf{R}) = -\text{Re} \int_{k=0}^{k_F} d\mathbf{k} \int_{k'=0}^{\infty} d\mathbf{k}' \frac{(\mathbf{w} \cdot (\mathbf{k}' + \mathbf{k}))^2 e^{i(\mathbf{k}' - \mathbf{k}) \cdot \mathbf{R}}}{(\hbar v_F (k' - k))^3} \tag{S40}$$

$$\begin{aligned}
&= \text{Re} \left(\int_{k=0}^{k_F} d\mathbf{k} \left(\frac{\mathbf{w}}{v_F} \cdot \frac{\partial}{\partial \mathbf{R}} \right)^2 e^{-i\mathbf{k} \cdot \mathbf{R}} \int_{k'=0}^{\infty} d\mathbf{k}' \frac{e^{i\mathbf{k}' \cdot \mathbf{R}}}{(\hbar v_F (k' - k))^3} \right) \\
&+ \text{Re} \int_{k=0}^{k_F} d\mathbf{k} e^{-i\mathbf{k} \cdot \mathbf{R}} \left[\left(\frac{\mathbf{w}}{v_F} \cdot \frac{\partial}{\partial \mathbf{R}} \right)^2 \int_{k'=0}^{\infty} d\mathbf{k}' \frac{e^{i\mathbf{k}' \cdot \mathbf{R}}}{(\hbar v_F (k' - k))^3} \right] \\
&+ 2\text{Re} \left[\left(\frac{\mathbf{w}}{v_F} \cdot \frac{\partial}{\partial \mathbf{R}} \right) \int_{k=0}^{k_F} d\mathbf{k} e^{-i\mathbf{k} \cdot \mathbf{R}} \right] \left[\left(\frac{\mathbf{w}}{v_F} \cdot \frac{\partial}{\partial \mathbf{R}} \right) \int_{k'=0}^{\infty} d\mathbf{k}' \frac{e^{i\mathbf{k}' \cdot \mathbf{R}}}{(\hbar v_F (k' - k))^3} \right].
\end{aligned} \tag{S41}$$

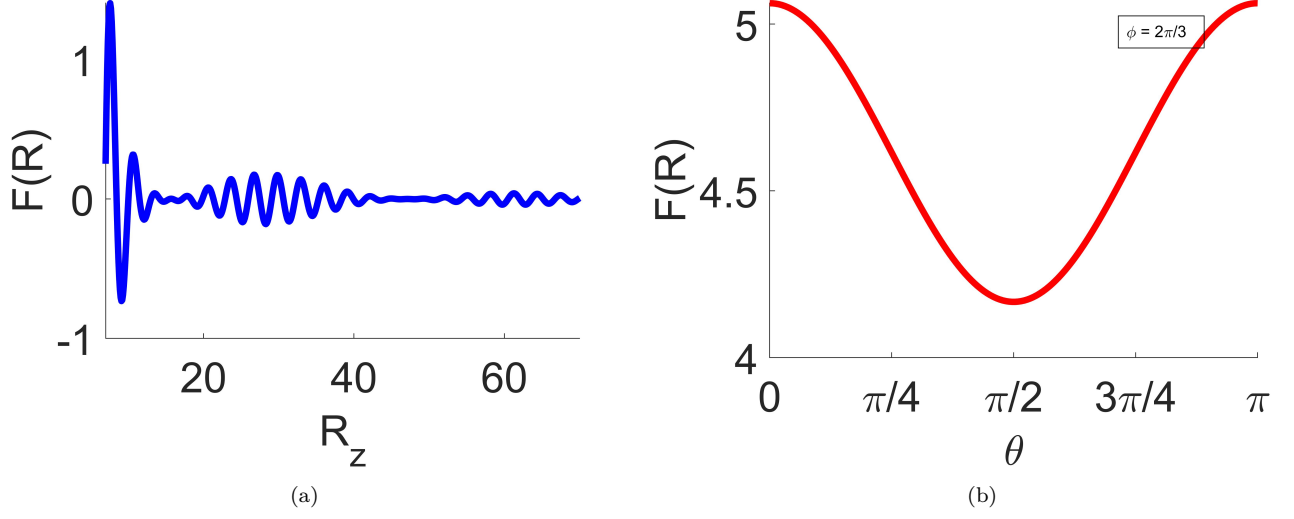


FIG. S1: IR breaking WSM: Plot of Range function w.r.t. (a) R_z when the tilt $\mathbf{w} \parallel \hat{z}$; (b) the angle $\theta = \angle(\mathbf{w}, \mathbf{R})$ when $\mathbf{w} \parallel \hat{z}$.

We calculate above but as the final expression is too large, we just show plot the results in manuscript. **IR-broken** ($\mathbf{Q} = 0$):

$$F(\mathbf{R}) = \left\{ \sum_{\eta} \chi^{(0,\eta)}(\mathbf{R}) - \sum_{\eta} \chi^{(2,\eta)}(\mathbf{R}) \right\} + \left\{ \sum_{\eta} \left[\xi^{(0,\eta,-\eta)}(q_0, \mathbf{R}) - \xi^{(2,\eta,-\eta)}(q_0, \mathbf{R}) \right] \right\}, \quad (\text{S42})$$

with

$$\begin{aligned} \zeta^{(2)}(\eta, -\eta, \mathbf{R}) &= -\mathbf{Re} \int_{k=0}^{k_{F\eta}} d\mathbf{k} \int_{k'=0}^{\infty} d\mathbf{k}' \frac{(\mathbf{w} \cdot (\mathbf{k}' + \mathbf{k}))^2 e^{i(\mathbf{k}' - \mathbf{k}) \cdot \mathbf{R}}}{(\hbar v_F (k' - k) \mp 2q_0)^3} \\ &= \mathbf{Re} \left(\left(\frac{\mathbf{w}}{v_F} \cdot \frac{\partial}{\partial \mathbf{R}} \right)^2 \int_{k=0}^{k_{F\eta}} d\mathbf{k} e^{-i\mathbf{k} \cdot \mathbf{R}} \right) \int_{k'=0}^{\infty} d\mathbf{k}' \frac{e^{i\mathbf{k}' \cdot \mathbf{R}}}{(\hbar v_F (k' - k) \mp 2q_0)^3} \\ &+ \mathbf{Re} \int_{k=0}^{k_{F\eta}} d\mathbf{k} e^{-i\mathbf{k} \cdot \mathbf{R}} \left[\left(\frac{\mathbf{w}}{v_F} \cdot \frac{\partial}{\partial \mathbf{R}} \right)^2 \int_{k'=0}^{\infty} d\mathbf{k}' \frac{e^{i\mathbf{k}' \cdot \mathbf{R}}}{(\hbar v_F (k' - k) \mp 2q_0)^3} \right] \\ &+ 2\mathbf{Re} \left[\left(\frac{\mathbf{w}}{v_F} \cdot \frac{\partial}{\partial \mathbf{R}} \right) \int_{k=0}^{k_{F\eta}} d\mathbf{k} e^{-i\mathbf{k} \cdot \mathbf{R}} \right] \left[\left(\frac{\mathbf{w}}{v_F} \cdot \frac{\partial}{\partial \mathbf{R}} \right) \int_{k'=0}^{\infty} d\mathbf{k}' \frac{e^{i\mathbf{k}' \cdot \mathbf{R}}}{(\hbar v_F (k' - k) \mp 2q_0)^3} \right], \end{aligned} \quad (\text{S44})$$

and,

$$\chi^{(2,\eta)}(\mathbf{R}) = \zeta^{(2)}(\eta, \eta', R) \Big|_{q_0=0}. \quad (\text{S45})$$

For the larger size of the expressions we do not show the expressions here.

$$\zeta_{IR}^{(2)}(\eta, -\eta, R) = -\mathbf{Re} \int_{k=0}^{k_{F\eta}} d\mathbf{k} \int_{k'=0}^{\infty} d\mathbf{k}' \frac{(\mathbf{w} \cdot (\mathbf{k}' + \mathbf{k}))^2 e^{i(\mathbf{k}' - \mathbf{k}) \cdot \mathbf{R}}}{(\hbar v_F (k' - k) \mp 2Q_0)^3} \quad (\text{S46})$$

using, $\mathbf{R} \cdot \mathbf{k} = Rx$, $\mathbf{R} \cdot \mathbf{k}' = Rx'$ and $\int d\mathbf{k} = \int dk k^2 \int d\theta \sin \theta \int d\phi = \int dk k^2 \int_{-1}^1 dx \int d\phi$,

$$\zeta_{IR}^{(2)}(\eta, -\eta, R) = -\text{Re} \left[\int_{k=0}^{k_F \eta} dk k^2 \int_{-1}^1 dx \int d\phi \right] \left[\int_{k'=0}^{\infty} dk' k'^2 \int_{-1}^1 dx' \int d\phi' \right] \frac{(\mathbf{w} \cdot (\mathbf{k}' + \mathbf{k}))^2 e^{i(\mathbf{k}' - \mathbf{k}) \cdot \mathbf{R}}}{(\hbar v_F (k' - k) \mp 2Q_0)^3}, \quad (\text{S47})$$

Now, rescale using, $\mathbf{k} \rightarrow (\mathbf{k} - \eta q_0 \hat{\mathbf{k}})$ and $\mathbf{k}' \rightarrow (\mathbf{k}' + \eta q_0 \hat{\mathbf{k}}')$ such that $\int_0^{k_F \pm} dk \rightarrow \int_0^{k_F} dk$ implies $k_F = k_{F\pm} \pm q_0$. As a result we rewrite,

$$\begin{aligned} & \zeta_{IR}^{(2)}(\eta, -\eta, R) \\ &= -\text{Re} \left[\int_{k=0}^{k_F} dk (k - \eta q_0)^2 \int_{-1}^1 dx \int d\phi \right] \left[\int_{k'=k_F}^{\infty} dk' (k + \eta q_0)^2 \int_{-1}^1 dx' \int d\phi' \right] \\ & \left[\frac{(\mathbf{w} \cdot (\mathbf{k}' + \eta q_0 \hat{\mathbf{k}}'))^2 + (\mathbf{w} \cdot (\mathbf{k} - \eta q_0 \hat{\mathbf{k}}))^2 + 2(\mathbf{w} \cdot (\mathbf{k}' + \eta q_0 \hat{\mathbf{k}}')) (\mathbf{w} \cdot (\mathbf{k} - \eta q_0 \hat{\mathbf{k}}))}{(k' - k)^3} \right] \\ & \times e^{i(\mathbf{k}' + \eta q_0 \hat{\mathbf{k}}' - \mathbf{k} + \eta q_0 \hat{\mathbf{k}}) \cdot \mathbf{R}}. \end{aligned} \quad (\text{S48})$$

Now, using $\mathbf{w} = w_x \hat{x} + w_y \hat{y} + w_z \hat{z}$ and $\mathbf{R} = \hat{z}R$,

$$\begin{aligned} & \zeta_{IR}^{(2)}(\eta, -\eta, R) \\ &= \text{Re} \left(\left(\frac{\mathbf{w}}{v_F} \cdot \frac{\partial}{\partial \mathbf{R}} \right)^2 \left[\int_{k=0}^{k_F} dk (k - \eta q_0)^2 \int_{-1}^1 dx \int d\phi \right] e^{-i(\mathbf{k} - \eta q_0 \hat{\mathbf{k}}) \cdot \mathbf{R}} \right) \\ & \left[\int_{k'=k_F}^{\infty} dk' (k + \eta q_0)^2 \int_{-1}^1 dx' \int d\phi' \right] \frac{e^{i(\mathbf{k}' + \eta q_0 \hat{\mathbf{k}}') \cdot \mathbf{R}}}{(k' - k)^3} \\ & + \text{Re} \left[\int_{k=0}^{k_F} dk (k - \eta q_0)^2 \int_{-1}^1 dx \int d\phi e^{-i(\mathbf{k} - \eta q_0 \hat{\mathbf{k}}) \cdot \mathbf{R}} \right] \\ & \left[\left(\frac{\mathbf{w}}{v_F} \cdot \frac{\partial}{\partial \mathbf{R}} \right)^2 \left[\int_{k'=k_F}^{\infty} dk' (k + \eta q_0)^2 \int_{-1}^1 dx' \int d\phi' \right] \frac{e^{i(\mathbf{k}' + \eta q_0 \hat{\mathbf{k}}') \cdot \mathbf{R}}}{(k' - k)^3} \right] \\ & + \text{Re} \left[\left(\frac{\mathbf{w}}{v_F} \cdot \frac{\partial}{\partial \mathbf{R}} \right) \left[\int_{k=0}^{k_F} dk (k - \eta q_0)^2 \int_{-1}^1 dx \int d\phi e^{-i(\mathbf{k} - \eta q_0 \hat{\mathbf{k}}) \cdot \mathbf{R}} \right] \right] \\ & \left[\left(\frac{\mathbf{w}}{v_F} \cdot \frac{\partial}{\partial \mathbf{R}} \right) \left[\int_{k'=k_F}^{\infty} dk' (k + \eta q_0)^2 \int_{-1}^1 dx' \int d\phi' \right] \frac{e^{i(\mathbf{k}' + \eta q_0 \hat{\mathbf{k}}') \cdot \mathbf{R}}}{(k' - k)^3} \right]. \end{aligned} \quad (\text{S49})$$

Writting, $\mathbf{R} \cdot \mathbf{k} = Rx$ and $\mathbf{R} \cdot \mathbf{k}' = Rx'$ and integrating over x, x' we obtain,

$$\begin{aligned} & \zeta_{IR}^{(2)}(\eta, -\eta, R) \\ &= \text{Re} \left(\int_{k=0}^{k_F} dk \left(\frac{\mathbf{w}}{v_F} \cdot \frac{\partial}{\partial \mathbf{R}} \right)^2 \frac{4\pi(k - \eta q_0) \sin(R(k - \eta q_0))}{R} \right) \left[\int_{k'=k_F}^{\infty} dk' \frac{4\pi(k' + \eta q_0) \sin(R(k' + \eta q_0))}{R(k' - k)^3} \right] \\ & + \text{Re} \left[\int_{k=0}^{k_F} dk \frac{4\pi(k - \eta q_0) \sin(R(k - \eta q_0))}{R} \right] \left(\frac{\mathbf{w}}{v_F} \cdot \frac{\partial}{\partial \mathbf{R}} \right)^2 \int_{k'=k_F}^{\infty} dk' \frac{4\pi(k' + \eta q_0) \sin(R(k' + \eta q_0))}{R(k' - k)^3} \\ & + \text{Re} \left[\int_{k=0}^{k_F} dk \left(\frac{\mathbf{w}}{v_F} \cdot \frac{\partial}{\partial \mathbf{R}} \right) \frac{4\pi(k - \eta q_0) \sin(R(k - \eta q_0))}{R} \right] \left(\frac{\mathbf{w}}{v_F} \cdot \frac{\partial}{\partial \mathbf{R}} \right) \left[\int_{k'=k_F}^{\infty} dk' \frac{4\pi(k' + \eta q_0) \sin(R(k' + \eta q_0))}{R(k' - k)^3} \right]. \end{aligned} \quad (\text{S50})$$

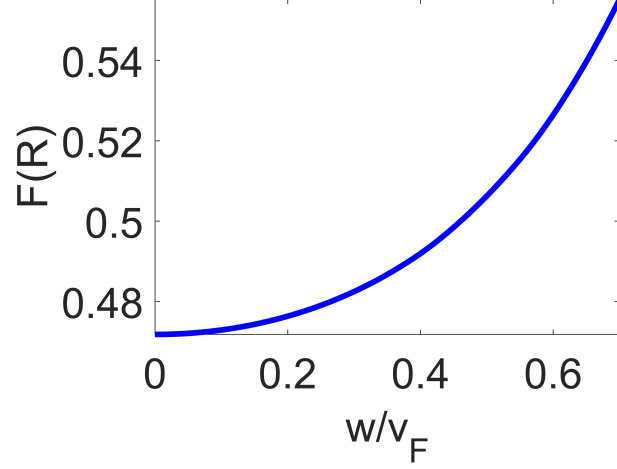


FIG. S2: Plot of Range function w.r.t. tilt magnitude \mathbf{w} for TRS breaking WSMs

IV. FINITE TILT LIMIT:

Thus far, we have considered the analytical expression of the RKKY range function in the small-tilt limit. In this section, we will analyze the RKKY range function numerically for any arbitrary tilt value. We will consider the general expressions in Eqs. (S6-S11) and assume parallel tilt vector for all Weyl nodes. In our calculations, we arbitrarily set the tilt as $\mathbf{w} \parallel \hat{z}$ and express the separation vector $\mathbf{R} = R(\sin(\theta) \cos(\phi)\hat{x} + \sin(\theta) \sin(\phi)\hat{y} + \cos(\theta)\hat{z})$. In Fig. S2, we plot the range function with respect to the tilt magnitude $|\mathbf{w}|$ for TRS broken case. The RKKY function has non-linear dependence on tilt, matching the trend of our analytical result.